Efficient, robust, and versatile fluctuation data analysis using MLE MUtation Rate calculator (mlemur)

Krystian Łazowski

Laboratory of DNA Replication and Genome Stability, Institute of Biochemistry and Biophysics of the Polish Academy of Sciences, Pawiński ego 5a, Warsaw 02-106, Poland

ARTICLE INFO	ABSTRACT
Keywords: Mutation rate Luria–Delbrück distribution Fluctuation assay Plating efficiency Phenotypic lag Cell death	The fluctuation assay remains an important tool for analyzing the levels of mutagenesis in microbial populations. The mutant counts originating from some average number of mutations are usually assumed to obey the Luria–Delbrück distribution. While several tools for estimating mutation rates are available, they sometimes lack accuracy or versatility under non-standard conditions. In this work, extensions to the Luria–Delbrück protocol to account for phenotypic lag and cellular death with either perfect or partial plating were developed. Hence, the novel MLE MUtation Rate calculator, or mlemur, is the first tool that provides a user-friendly graphical interface allowing the researchers to model their data with consideration for partial plating, differential growth of mutants and non-mutants, phenotypic lag, cellular death, variability of the final number of cells, post-exponential-phase mutations, and the size of the inoculum. Additionally, mlemur allows the users to incorporate most of these special conditions at the same time to obtain highly accurate estimates of mutation rates and *P* values, confidence intervals for an arbitrary function of data (such as fold), and perform power analysis and sample size determination for the likelihood ratio test. The accuracy of point and interval estimates produced by mlemur against historical and simulated fluctuation experiments are assessed. Both mlemur and the analyses in this work might be of great help when evaluating fluctuation experiments and increase the awareness of the limitations of the widely-used Lea–Coulson formulation of the Luria–Delbrück distribution in the more realistic biological contexts.

1. Introduction

1.1. The concept of measuring mutagenesis in microorganisms

In microbial genetic studies, researchers are often compelled to estimate the mutation rate, that is, the pace at which mutations are accumulated within the genome under certain conditions in a given genetic background and specific organism. Genetic mutations can arise, i.a., during DNA replication, DNA repair, or upon exposure to certain endo- and exogenous agents that chemically change the identity of the nitrogenous base within the nucleotide [1,2]. Whatever the mechanism, the mutation rate in a specific genetic background can often be informative of the underlying biological processes that affect the fidelity of DNA replication or the effectiveness of DNA repair.

Numerous assays have been developed to score mutagenesis. A modern approach to this problem is deep sequencing of genomic DNA of colonies that underwent multiple passages and accumulated mutations after hundreds of generations [3]. This method is precise because it is more robust against selecting only certain groups of mutations (for example, silent mutations can be observed). Moreover, it allows analyzing not only the rate but also the specificity of occurring mutations. On the other hand, mutation accumulation assays are time-consuming, laborious, and expensive. Other methods of measuring the mutator phenotype are based on counting the number of mutant cells that acquired a selectable mutation in a certain reporter gene, either before, during, or after the culture/colony growth. These mutants can be sorted and counted in flow cytometry (e.g., mutations in the gene encoding green fluorescent protein (GFP) can be scored with the usage of fluorescence-activated cell sorting [4]), but most usually are plated, allowing mutant colonies to be counted on a solid medium containing a selective agent (usually an antibiotic, a carbon source, or an amino acid).

These experiments usually start with several small parallel cultures of a given microorganism, grown to saturation under specified conditions. After growth, the whole, or a portion of, culture is plated onto the solid medium containing some selective agent. A small portion (usually a dilution) of all or only selected cultures is plated on a non-selective medium to estimate the population size in each sister culture. After that, the plates are incubated until visible colonies are formed [5].

Nomenclature

LD distribution	Luria–Delbrück distribution
LC distribution	Lea–Coulson distribution
MLE	maximum likelihood estimate
CI	confidence interval
PMF	probability mass function
CDF	cumulative distribution function
LRT	likelihood ratio test

Since with this approach, mutations are not observed directly, but rather by their effect on cell physiology (i.e., the ability to grow on selective medium), to infer conclusions about the mutation rate from the number of mutants on the plate, a certain statistical model must be applied. This is caused by the fact that the population of mutant cells (as well as non-mutants) grows exponentially, and the final number of mutants in the culture depends not only on the mutation rate but also on the time the mutation happened, and on how many divisions (generations) the mutant cell underwent afterward (Fig. 1A). This type of experiment is the oldest approach to mutation rate scoring and historically has been called a fluctuation assay. The first fluctuation assay was described by Salvador Luria and Max Delbrück in 1943 and eventually inspired generations of biostatisticians and microbiologists to pursue novel, more precise and accurate methods of measuring mutagenesis in living cells. To this day, fluctuation assay is a commonly used tool to estimate mutation rates in bacterial and eukaryotic microorganisms and some human cell lines.

Mutations occurring in a unperturbedly growing microbial culture are typically modeled by the Luria–Delbrück (LD) distribution [6], sometimes called Lea–Coulson (LC) distribution, to acknowledge their

big contribution to the topic [7]. Because there are no explicit expressions for the mean and the standard deviation of the Luria–Delbrück probability distribution, it is a common practice to use approximate methods such as the Jones method of the median, the Lea–Coulson method of the median, Drake formula, and methods based on the mean number of mutants (reviewed in [5]). Since there is a finite probability that a selectable mutation will occur quite early during culture growth, giving rise to an exceptionally big number of mutants on the plate (so-called 'jackpot' culture), the mutant distribution is heavy-tailed, and therefore methods of mutation rate calculation based on the mean number of mutant cells per plate are significantly biased; so are, although to a somewhat lesser extent and particularly with small samples, methods based on the median [8]. Sometimes scientists are confined to reporting only mutant frequency (often incorrectly called mutation frequency), that is, the average number of mutants observed per some number of cells. Mutant frequency, however, is not a biological property and strongly depends on the number of generations the culture underwent. Because of that, mutant frequencies measured by different protocols are not comparable and are not informative about the number of mutations that led to the observed number of mutants (Fig. 1A, B) [8, 9].

1.2. The Luria–Delbrück distribution and the fluctuation protocol

The Luria–Delbrück mutant distribution arises from combining several simple ideas. The basis of the derivation that is easy to follow was developed by Stewart et al., and it will be presented here [10,11]. First, we assume that the non-mutant cells grow deterministically (without randomness) but non-synchronously, according to a well-known equation for exponential growth:

$$N_t = N_0 e^{\beta t} \tag{1}$$

where N_0 is the size of the inoculum, β is the growth rate of the cells, and
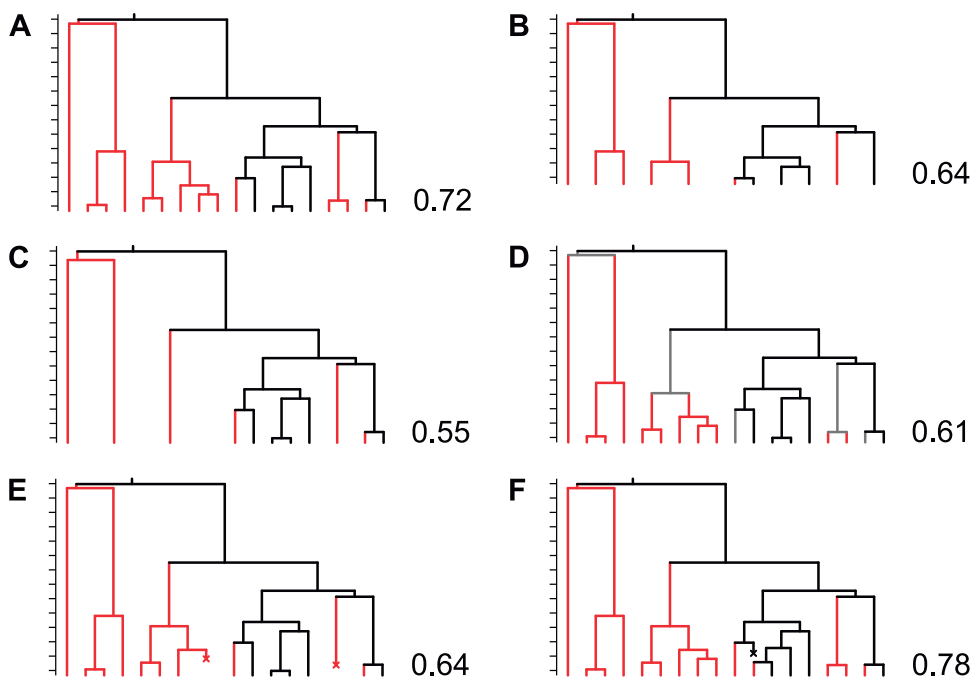
Fig. 1. The graphs depicting the interplay between the number of mutations and the proportion of mutant cells in the culture under different conditions. Data were simulated using the draw.clone function from R package flan assuming exponential cell lifetimes, $t = 3$, and mutation probability $= 0.5$. The proportion of mutants in the culture is presented next to each graph. Black lines: wild-type cells. Red lines: mutant cells. Gray lines: mutant cells that have not yet expressed mutant phenotype. Tilted cross: cell death. (A) The observed number of mutant cells depends on the stage at which the mutation occurred. While most mutations are expected to occur late during exponential growth of the culture (because most cell divisions happen at this time), the "early" mutations lead to the presence of so-called "jackpot" cultures with an exceptionally high number of mutant colonies. (B) If the growth of the culture were interrupted at an earlier moment, the produced mutant frequency would be lower (0.64 vs. 0.72) despite the constant mutation rate. (C) The observed mutant colony count depends on the growth rate of the mutant cells relative to the growth rate of the non-mutant cells. Here, due to the mutant growth rate being equal to half the growth rate of the non-mutant cells, the mutant frequency is 0.55. (D) The presence of a phenotypic lag decreases the observed mutant colony count. Here, with a phenotypic lag equal to one generation, the two last mutations produce cells that fail to grow on a selective medium because the mutant phenotype is not expressed at the time of plating (proportion of mutants 0.61). (E) Death of a mutant cell decreases the mutant count (mutant frequency 0.64). (F) However, the death of a non-mutant cell increases the number of cellular divisions needed to reach a given culture size, inflating the mutant count (mutant frequency 0.78).

t is the time we take the measurement of N_t. In the context of mutation rate estimation with the usage of the fluctuation protocol, the only time that is of interest is usually the time when the culture stopped growing, so we can equate t with the time when we interrupted culture growth and N_t with the size of the culture at this time. The exact value of t and β is not important because they are implicitly but unequivocally described by N_t.

The stochastic process of mutation is modeled as an inhomogeneous Poisson process whose intensity function $\lambda(t)$ is equal mutation rate per cell per time unit, times the size of the population at time t: $\lambda(t) = aN_t = aN_0 e^{\beta t}$. In other words, mutation is a rare event, and the chance of mutation at any given moment increases exponentially with time, proportionally to N_t. The actual number of mutations occurring between $\tau = 0$ and $\tau = t$ is a Poisson-distributed random variable with mean

$$\mathbb{E}[m(t)] = \int_0^t \lambda(\tau)d\tau = \int_0^t aN_0 e^{\beta\tau}d\tau = \frac{a}{\beta}N_0(e^{\beta t} - 1) = \mu(N_t - N_0). \quad (2)$$

(See (2) and (3) in [12]). The parameter $\mu = a/\beta$ that made appearance in the above equation is the unitless mutation rate per cell division we are interested in estimating. There are two important pieces of information to give at this point. First, for large t, the expectation of m can be replaced with the actual count of m. Second, while the number of cell divisions is $N_t - N_0$, the size of the inoculum is usually of the order of magnitude 10^2–10^3 and the usual final culture size has the order of magnitude 10^8–10^9. Therefore, in most cases we can ignore N_0, and hence:

$$\mu = \frac{\mathbb{E}[m(t)]}{N_t - N_0} \approx \frac{m(t)}{N_t}. \quad (3)$$

Consequently, we arrive at the usual expression for mutation rate per cell division. Importantly, μ does not depend on the growth rate of the cells. It is assumed that this form of mutation rate does not change when the growth rate changes. The same assumption is used throughout this paper. The mutation rate per unit of time (here denoted by a) can be obtained by multiplying (3) by the independently estimated growth rate of the strain, although it is rarely reported. Multiplication by other factors (2 or logarithm of 2), which were proposed by Luria & Delbrück [6] and Armitage [13], has been discouraged [14].

The problem at hand is how to retrieve the number of mutations $m = \mu N_0 e^{\beta t}$ from the number of mutants on the plate. If we consider a very short period dt, during which there are dN cell divisions, then the chance of a mutation occurring between t and $t + dt$ is given by the differential

$$\mu N_0 e^{\beta t}\beta dt. \quad (4)$$

Now, let us say that at some point during culture growth, a mutation arose: one wild-type cell divided into one wild-type cell and one mutant cell. If this mutation arose at some time τ before t, then the mutant cell has time $t - \tau$ to proliferate. We could model the dynamics of the mutant cells using the same equation (1), as this was done originally by Luria and Delbrück, but their growth is frequently taken as random. A stochastic process similar to the deterministic exponential growth process is called the Yule process, or the pure birth process, in which the chance of a single mutant cell growing to a clone of size $n \geq 1$ between the time mutation happened τ, and the time the culture stopped growing t is given by (equation (8.15) in Bailey 1964 [15])

$$e^{-\beta(t-\tau)}[1 - e^{-\beta(t-\tau)}]^{n-1} \quad (5)$$

which is also an expression for the probability mass function of the geometric distribution with $p = e^{-\beta(t-\tau)}$. In the Yule process, the lifetimes of individual cells are exponentially distributed with the mean equal β. For large t, deterministic and stochastic models give asymptotically equivalent results [16]. If we now extend our considerations to the whole time of the culture growth from the beginning to the end at time t, the mean number of mutations giving rise to $n \geq 1$ colonies is

given by the integral of the product of equations (4) and (5) over the whole time of culture growth, that is,

$$\lambda_n = \int_0^t \mu N_0 e^{\beta\tau}\beta e^{-\beta(t-\tau)}[1 - e^{-\beta(t-\tau)}]^{n-1}d\tau. \quad (6)$$

Evaluation of the above with some approximations explained later leads to the classic formulation of the Luria–Delbrück distribution by Lea and Coulson ((25) in [10]):

$$\lambda_n \approx \frac{m}{n(n+1)}. \quad (7)$$

$\{\lambda_n\}$ can be interpreted as follows: the number of mutations resulting in a clone of size $n \geq 1$ is a Poisson-distributed random variable with the Poisson parameter (mean) λ_n. $\{\lambda_n\}$ can be used to derive a formula for the probability distribution of the total number of mutants in the culture provided that, on average, m mutations occurred, i.e., the LD distribution.

At this moment, it is worth pointing out that in (3), we conveniently overlook that in a real-world scenario, we replace N_t with the average culture size, which contains both wild-type and mutant cells. The actual number of wild-type cell divisions is smaller than the culture size that is estimated by plating on non-selective medium. Because the estimate of N_t usually has only 3 significant digits, the additional inaccuracy introduced by ignoring mutant cells (similarly to neglecting inoculum) when calculating the number of divisions is minuscule, so $N_t + n \approx N_t$. (It needs to be noted that this n, denoting the number of mutants, is different from n in (5), (6), and (7), as in those equations n represents the size of the clone). However, for this reason, the mutant cell population relative to N_t should be kept small so that the error does not grow out of control.

The Luria–Delbrück mutant distribution is merely an approximation of a complex biological process. As a consequence of the model, a classic fluctuation assay has a set of assumptions: cells (a) grow exponentially and (b) independently from each other with (c) no death events (d) from an inoculum that is miniscule in size compared to the final culture; mutations occur (e) at the moment of cell division (f) at a low and (g) constant rate from the time the culture growth started until it stopped, (h) are not influenced by previous mutations, (i) do not revert, (j) do not occur after culture growth has stopped (either in the stationary phase or after plating), are (k) immediately expressed, and (l) result in creation of only one mutant cell (this refers to the moment of mutation and should not be confused with further proliferation of this single initial mutant cell); mutant cells (m) have life-times that obey the exponential distribution, (n) constitute a small portion of the whole culture, (o) have comparable fitness to non-mutant cells, and (p) are always detected; (q) parallel cultures are homogenous in terms of volume and size.

While most of the conditions imposed by the Luria–Delbrück model can be easily met, many commonly used fluctuation protocols do not strictly meet its criteria. The requirement that the cells are in the exponential growth phase is commonly violated. The cultures are usually grown to saturation (frequently overnight); therefore, the cells undergo growth deceleration and eventually enter the stationary phase. How this affects the presumptive constancy of mutation rate during growth is not well understood; it is known, however, that some unicellular organisms entering the stationary phase activate SOS-induced DNA polymerases and accumulate mutations that increase their fitness under conditions of nutrient depletion [17–19].

In the above example, the potential conflict between assumptions and protocol can be circumvented by interrupting the culture growth when cells are still in the exponential phase. However, there are many situations where deviations from the fluctuation criteria are not quite in the researcher's hands. For instance, forward mutations in *rpoB* affect the structure of bacterial RNA polymerase; therefore, they are non-neutral regarding cellular fitness and can affect growth rate to a different extent depending on the genetic background (Fig. 1C) [20].

Stress-induced mutagenesis due to the presence of a sub-inhibitory antibiotic concentration during culture growth can increase the death rate of wild-type cells, and so can certain genetic backgrounds that severely impact cellular growth (such as mismatch repair deficiency). Mutations in carbon source metabolism-associated genes such as *lacZ* can occur after plating due to adaptive mutagenesis because the selective agent does not immediately kill the non-mutant cells [21,22]. A phenotypic lag (the phenomenon of delayed expression of a scorable phenotype post mutation due to the necessity to accumulate mutant protein product at a sufficient level) is also widespread with mutations causing antibiotic resistance, yet rarely accounted for (Fig. 1D) [23,24]. Finally, an elevated mutation rate can force the researcher to plate only a portion of the culture on a selective medium. Because of that, not all mutant cells will be directly detected (imperfect plating or plating efficiency less than 100 %). While, in theory, in the last example, the researcher can stop the culture growth when mutant cells are still countable, this might violate the assumption that the final number of cells in culture is much bigger than the starting cell count.

The method of choice for estimating mutation rates by employing the Luria–Delbrück distribution is the maximum likelihood estimation (MLE) [5]. MLE is a statistical tool for finding the value of some parameter of a statistical distribution for which the data are most likely to be observed (drawn from). Based on numerous simulations, maximum likelihood-based methods are the most accurate of all available tools for mutation rate estimation under the Luria–Delbrück protocol [9,25–27]. The popularity of the MLE method can be attributed to Ma, Sandri, and Sarkar, who developed recursive algorithms for efficient computation of the values of the probability mass function (PMF) [28, 29], as well as tremendous work of Qi Zheng with SALVADOR [12,30].

Among significant contributions that allowed to relax some of the strict conditions imposed by the fluctuation protocol that the researcher cannot easily mitigate are the works of: Armitage, who proposed the adjustment for imperfect (not 100 %) plating based on binomial thinning (this work was later extended by Crane, Jones, Stewart, Gerrish, Zheng) [11,13,25,31–34,35]; Angerer, who derived modifications for the phenotypic delay and the presence of residual mutations (the subject was also studied by Armitage, Koch, Mandelbrot, Newcombe, Crump et al., and Stewart et al.) [10,13,16,23,36–38]; Mandelbrot, Koch, Jones, and Stewart, found analytical solutions that allow accounting for differential growth of mutant and non-mutant cells (a model that takes into account the relative fitness of the mutant cells compared to non-mutants has been named Mandelbrot–Koch model, see Fig. 1C), also with imperfect plating [11,34,36,37]; Zheng, who developed the model allowing to correct for the variation between population sizes in parallel sister cultures (a gamma mixture of the LD distribution, sometimes called the B^0 distribution) [39–42]. Kendall, Zheng, Stewart, Angerer, and Dewanji et al. have also considered increased cell death and the effect of the size of the inoculum [43,10,30,44–46]. Dewanji et al. proposed an alternative solution to the mutant birth-and-death model, which considers deceleration at the late phase of culture growth. The occurrence of residual mutations is easy to account for if the expected number of post-plating mutants is known, but this, in turn, is hard to quantify in practice. It has been proposed that adaptive mutagenesis on lactose plates may be limited by using scavenger and filler strains and incubating the plates for as short a period as possible [22].

1.3. Tools for estimating mutation rates

Several tools for mutation rate estimation are currently available: bz-rates [47] and flan [48], both using the so-called empirical generating function (GF) method and asymptotical normality assumption, as well as rSalvador [27] and FluCalc [49] based on the maximum likelihood (ML) method. bz-rates is an online tool, whereas flan and rSalvador are free packages for an open statistical analysis language R, and FluCalc is written in Python. flan and rSalvador have their online versions available at http://shinyflan.its.manchester.ac.uk and https://websalvador.

eeeeeric.com, respectively. A popular tool for estimating mutation rates is FALCOR [50], available at https://lianglab.brocku.ca/FALCOR/index.html, which also uses the ML method. Based on simulations, rSalvador is the most accurate. However, it does not exactly meet our needs. Here, a novel tool for fluctuation data analysis is introduced: MLE Mutation Rate Calculator, or mlemur.

Based on the frameworks developed by Qi Zheng, mlemur allows the user to obtain point and interval estimates of mutation rates, compare two datasets using the likelihood ratio test to calculate *P* values and adjust computed *P* values using either Bonferroni, Bonferroni–Holm, or Benjamini–Hochberg corrections, estimate the power and the sample size for the likelihood ratio test, and compute confidence intervals (CIs) for an arbitrary function of mutation rates.

Unlike flan and rSalvador, mlemur is almost entirely typing–free: after initialization via the mlemur::mlemur() command in R, all control is done from within the web browser window. At every stage, mlemur provides the user with information about the type of input required in each data field and feedback when an error occurs. Users can also load their data from an XLS(X) file to simultaneously compute mutation rates, confidence intervals, and *P* values (adjusted or not) for a whole set of strains. At last, with a single click, researchers can download the results in a spreadsheet format. Additional options for calculating mutation rates and *P* values for paired data (colony counts on selective and non-selective medium for each culture), finding confidence intervals for an arbitrary function (such as fold or difference) of mutation rates, estimating statistical power (the probability that true differences will be discovered), and determining sample size to achieve a prescribed level of power of the likelihood ratio test, have been implemented.

With mlemur, one can calculate mutation rates using a handful of options:

- the standard Lea–Coulson model (approximate Luria–Delbrück distribution) with almost all the previously mentioned assumptions in place but overlooking the impact of the inoculum,
- the exact Luria–Delbrück distribution with consideration for the size of the inoculum,
- the compound LC–gamma model (B^0 distribution), which accounts for variability in culture sizes,
- the Mandelbrot–Koch model with differential growth of mutants and non-mutants,
- the stochastic modification of Angerer's model where the phenotypic delay is present,
- the Birth–Death (BD) model with cell death,
- the Poisson–LC convolved distribution where post-plating residual mutations are anticipated.

A unique feature of mlemur is that it allows the user to combine most of these generalizations when modeling their data with either perfect or partial plating. This is especially handy when one scores for multiple phenotypes at once or when dealing with particularly strong mutators.

Additionally, the functions for simulating fluctuation experiments and calculating mutation rates using various historical methods have been implemented and are available from the R console in mlemur. The mathematical background for all developments can be found in Supplementary File S1, but the most relevant derivations will also be available in the following sections.

In this work, I present the possibilities of mlemur and derive new formulas for some extensions of the Luria–Delbrück protocol. I focus on the practical application of the Luria–Delbrück model to estimate mutation rate from simulated and real-world data, investigating the accuracy and confidence interval coverage of point and interval estimates.

2. Materials and methods

2.1. Algorithms for maximum likelihood estimation

The algorithms used in this work for estimating mutation rates are a part of the free R statistical package mlemur, available at https://github.com/krystianll/mlemur. They are also described in detail in Supplementary File S1.

2.2. Simulating fluctuation experiments

Most of the work presented here was done by analyzing simulated fluctuation experiments. The simulation algorithm that is a part of mlemur combines previously used approaches with the novel addition of phenotypic lag [41,42,48]. The outline of the simulation of a single test tube is presented here:

- The final culture size is taken either as a constant or as a random variable drawn from a gamma distribution.
- Growth (and death if applicable) of the non-mutant cells is assumed to be deterministic and exponential. The time of culture growth is calculated per tube using the starting and the final numbers of cells and the non-mutant death rate. The average number of mutations, which is proportional to the number of cellular divisions, is calculated using the average mutation rate, the growth rate, the death rate, and the time of culture growth.
- The actual number of mutations in the test tube is drawn from a Poisson distribution using the average number of mutations from the previous step.
- The mutation event times (expressed in terms of the number of individual cell divisions at that moment as a fraction of the total number of cell divisions at the end of culture growth) are drawn from a uniform distribution, and then mutation epochs are calculated. For each mutant clone, the length of phenotypic lag is drawn from a Poisson distribution, with the mean being the average length of phenotypic lag (supplied as the number of generations, with a 'generation' defined as the mean time required for the population size to double, $\log(2/\beta)$. If a particular mutation epoch exceeds the total time of culture growth minus the extent of phenotypic lag, the mutant lineage is discarded.
- The size of the mutant clone is drawn from the distribution of the number of cells in a simple birth-and-death process using (8.46) in Bailey 1964 [15].
- If the plating is imperfect, the number of mutant colonies on the plates is drawn from a binomial distribution.

To simulate the mutant counts under the protein dilution model, a slightly modified version of the code used by Barna was used [51].

The code for simulating a fully stochastic Bartlett mutation model is an evolution of the Renshaw algorithm described by Zheng [41,46], available at https://github.com/eeeeeric/rSalvador/blob/master/python-examples/simuKessler.py.

3. Results and discussion

3.1. The probability distribution induced by the Luria–Delbrück model

The probability distribution induced by considerations from the Introduction can be written concisely ((18) in [10])

$$\sum_{n=0}^{\infty} p_n z^n = \exp\left[-m + \lambda_0 + \sum_{n=1}^{\infty} \lambda_n z^n\right]. \tag{8}$$

Here λ_n is the expected number of mutations that produce a clone of size n, which in the case of a simple Luria–Delbrück model, is given by (6). It is, however, convenient to re-cast the above as (see Lemma 2 in [12])

$$\sum_{n=0}^{\infty} p_n z^n = \exp\left\{m \sum_{n=0}^{\infty} h_n z^n\right\}. \tag{9}$$

In this form, the auxiliary sequence $\{h_n\}$ is independent of m. Calculating the values of the probability mass function (PMF) comes down to calculating the values of the auxiliary sequence, which needs to be done only once and can be reused for different values of m in each iteration when the MLE of m is found numerically by maximization of the likelihood function.

The formula for $\{h_n\}$ obtained by evaluating (6) exactly is given by

$$\left.\begin{array}{l} h_0(\varphi) = -1 \\ h_n(\varphi) = (1-\varphi)^{n-1} \dfrac{1+\varphi n}{n(n+1)} \text{ for } n \geq 1 \end{array}\right\}, \tag{10}$$

with $\varphi = N_0/N_t$ (see (7) in [52]). The Lea–Coulson simplification used to obtain (7) was to neglect inoculum by substituting $\varphi = 0$, in which case we arrive at

$$h_n = \frac{1}{n(n+1)} \quad \text{for } n \geq 1. \tag{11}$$

In the following sections, formulas for $\{h_n\}$ will be shown when some of the assumptions of the Luria–Delbrück model are violated. Unless stated otherwise, in all these cases it will be assumed that $\varphi = 0$, as in the LC formulation. Many of these formulas were already presented in the literature. I also present simulation-based studies and, in some cases, real-world examples of how violation of these assumptions affects the mutant distribution and, consequently, estimation of the mutation rates.

3.2. Plating a part of the culture

One of the most important deviations from the Luria–Delbrück model concerns plating only a fraction of the culture. A parameter defined as the fraction of culture plated is called plating efficiency, ε. As argued in [27], mutant cells are not uniformly dispersed throughout the culture, and sampling introduces an additional element of chance. From a statistical point of view, upon sampling, each mutant cell undergoes an independent Bernoulli trial with the probability of success (forming a colony) equal ε. This is best understood if we consider a culture containing a single mutant cell. If we plate half of this culture, the mutant cell has a 50 % chance of being plated. If the culture contains 2 mutant cells, then each of these cells will be plated with a 50 % probability: we might expect that one mutant cell will be plated, but it is also possible that we plate 0 or 2 because plating of one cell does not influence the probability of another cell being plated. Armitage was the first to propose to model partial plating using the binomial distribution (see (50) in [13]). By multiplying (6) by the expression for the PMF of the binomial distribution, we can arrive at the formula for the expected number of mutations producing $k \geq 1$ mutants, of which $n \geq 0$ are observed (equation (4) in [25]):

$$\int_0^t \binom{k}{n} \varepsilon^n (1-\varepsilon)^{k-n} \mu N_0 e^{\beta\tau} \beta e^{-\beta(t-\tau)} \left[1 - e^{-\beta(t-\tau)}\right]^{k-1} d\tau. \tag{12}$$

Based on the work of Stewart and Zheng [10,11,25], the formula for $\{h_n\}$ with imperfect plating assumes the form

$$\left.\begin{array}{l} h_0(\varepsilon) = \zeta \log \varepsilon \\ h_1(\varepsilon) = \zeta \left(-1 - \dfrac{\log \varepsilon}{1-\varepsilon}\right) \\ h_n(\varepsilon) = \zeta \left(\dfrac{1}{n(n-1)} - h_{n-1}(\varepsilon)\right) \text{ for } n \geq 2 \end{array}\right\}, \tag{13}$$

with

$$\zeta = \frac{\varepsilon}{1-\varepsilon}.$$

Due to the random nature of sampling, approaches based on dividing either colony counts or an intermediate estimate m^* obtained assuming perfect plating by the plating efficiency parameter to return the true number of mutants in culture or true value of m, respectively, will inescapably fail. Fig. 2 corroborates the intuitive notion that plating a portion of size ε of a culture with the average number of mutations m_1 and plating whole culture with the average number of mutations $m_2 = \varepsilon m_1$ give completely different distributions of colony counts. Another popular correction for imperfect plating was proposed by Stewart (equation (41) in [10]):

$$m = m^* \frac{\varepsilon - 1}{\varepsilon \log \varepsilon}. \tag{14}$$

As was shown by Zheng, Stewart's correction gives acceptable point estimates only for large values of ε [25]. However, even then, applying it to confidence limits will usually render the more important interval estimates outside nominal coverage (Table 1).

Expectedly, sampling from culture comes with a trade-off: the lower the plating efficiency, the wider the confidence interval, and to control the loss of precision of estimation, the experimentalist must set up a higher number of parallel cultures (Table 1, column: Armitage correction – median CI width).

The popular tool for mutation rate estimation, FALCOR, cannot correctly handle the cases when $\varepsilon < 1$. Firstly, the authors propose normalizing the colony counts to 1 ml of the culture, which is invalid for the reasons explained above. In the column "Rosche and Foster" in Table 1, m was estimated by first dividing colony counts by ε to obtain a theoretical number of mutant cells in the whole culture and then using these new colony counts to compute MLE with the assumption $\varepsilon = 1$. This approach gives acceptable results for bigger values of ε, whereas for $\varepsilon = 0.1$, m is underestimated by ~ 24 % (Table 1, column: Rosche and Foster – median m). The underestimation is heavily influenced by cultures with 0 mutant cells. Secondly, FALCOR utilizes the following formula proposed by Rosche and Foster to calculate approximate 95 % confidence intervals [5]:

$$CL_{95\%} = \exp[\log(m) \pm 1.96\sigma (e^{1.96\sigma})^{\mp 0.315}],$$

with

$$\sigma \approx \frac{1.225 m^{-0.315}}{\sqrt{C}},$$

and C being the number of cultures. This method works well when the

departure from the classical Lea-Coulson model is small, i.e., when the whole or a big part of the culture is plated. Comparison of the coverage of CIs produced using an inverted likelihood ratio test with these obtained using Rosche and Foster method shows that the latter are non-conservative, especially for very low values of ε because the loss of precision caused by partial plating is not accounted for (Table 1, column: Rosche and Foster – CI coverage).

3.3. Differential growth of mutants and non-mutants

An important limitation of the classic Luria–Delbrück model is that it requires the mutant cells to have the same growth rate as the wild–type cell. However, when measuring the mutagenesis of the reporter genes that are also essential for the functioning of the cell (such as *rpoB* or *gyrA* in the case of *E. coli*), one may expect that the mutations, while favorable during growth on the selective media containing Rif or Nal, might be disadvantageous when cells are not exposed to the selective agent [53].

As far as mutation rates are of concern, accounting for the differential growth rate of mutant and wild-type populations requires only knowledge about their relative fitness. Therefore, even a simple strategy of estimating the fitness of two competitors, namely competition assay, will suffice. Another popular fitness assay is, e.g., the estimation of the maximum growth rate from OD measurements (reviewed in [54]).

To make things more troublesome, *rpoB* has around eighty mutational sites [55], with different classes of substitutions and sequence contexts; each site may affect cell growth to a different extent. One *E. coli* study with 8 different *rpoB* mutations showed that the relative fitness could lie anywhere between 0.7 and 1.0 [56]. Similar studies were conducted in other bacteria [57–59]. It is unclear how variability in the mutant fitness affects mutant distribution and accuracy of mutation rate estimation.

The generalization of the Lea–Coulson model that allows mutant cells to grow at a different rate than non-mutant cells is often called Mandelbrot–Koch model [30,36,37]. Under this formulation, $\{h_n\}$ can be written as follows:

$$\left. \begin{aligned} h_0(r) &= -1 \\ h_1(r) &= \frac{r}{1+r} \\ h_n(r) &= \frac{n-1}{n+r} h_{n-1}(r) \text{ for } n \geq 2 \end{aligned} \right\}, \tag{15}$$

with r being the relative growth rate of non-mutants compared to mutants. The reciprocal value $\rho = 1/r$ is defined as the relative growth of mutants to non-mutants. It is easily checked that when substituting $r = 1$, one arrives at the Lea–Coulson formulation.

Solution for the case $\varepsilon \neq 1$ has been found by Stewart and reiterated by Jones [11,34]:

$$\left. \begin{aligned} h_0(r, \varepsilon) &= -1 + \frac{r(1-\varepsilon)}{r+1} \mathbf{F}(1, 1; r+2; 1-\varepsilon) \\ h_n(r, \varepsilon) &= r e^r \mathbf{B}(n, r+1) \mathbf{F}(r, r+1; r+1+n; 1-\varepsilon) \text{ for } n \geq 1 \end{aligned} \right\}. \tag{16}$$

Here, $\mathbf{B}$ is the beta function, and $\mathbf{F}(a, b; c; z)$ is the Gauss hypergeometric function. To save computational time $\{h_n\}$ can be computed using recursive formulas provided in the Supplemental Information.

The impact of differential fitness is most significant in the case of early mutants, which produce more offspring (Fig. 1C, Fig. 3). For example, a lower mutant growth rate results in lower jackpot colony counts and, therefore, lower variance. As a side note, when $r \longrightarrow \infty$ (and therefore $\rho \longrightarrow 0$), the mutant distribution asymptotically becomes the Poisson distribution. Table 2 shows that when r and ε are correctly accounted for, both point and interval estimates are accurate for various parameter values.
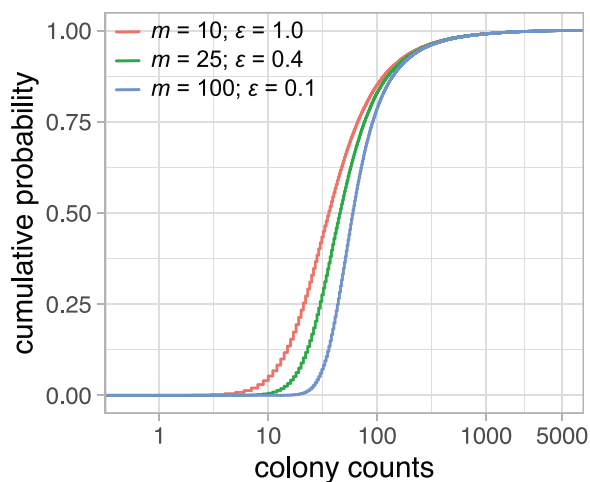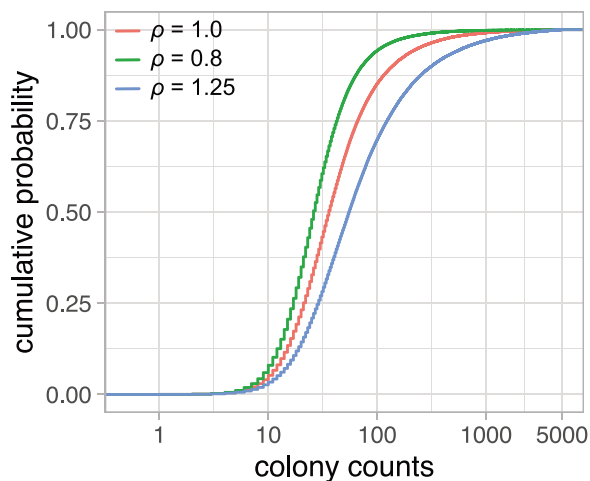

Fig. 2. Empirical CDFs of mutant counts under different plating efficiency parameters. One 100,000-tube experiment was simulated for each case. For picture clarity, only the values of the CDF up to the colony count of 5000 are shown. Red – $m = 10$, $\varepsilon = 1$; green – $m = 25$, $\varepsilon = 0.4$; blue – $m = 100$, $\varepsilon = 0.1$.

Table 1

Analysis of point and interval estimates for different values of plating efficiency.

Simulation parameters				Armitage correction			Stewart correction			Rosche and Foster (FALCOR)		
N_E	n_C	m	ε	median m	CI coverage	median CI width	median m	CI coverage	median CI width	median m	CI coverage	median CI width
10000	30	50	0.8	50.3	94.7 %	29.4 %	47.4	88.3 %	30.1 %	50.1	90.4 %	25.5 %
10000	30	10	0.8	10.0	94.7 %	42.7 %	9.62	93.9 %	43.5 %	9.84	93.6 %	42.5 %
10000	30	10	0.4	10.0	95.1 %	45.6 %	8.72	81.0 %	48.8 %	9.58	89.2 %	42.8 %
10000	30	10	0.1	10.0	95.6 %	57.4 %	8.13	76.8 %	63.3 %	7.60	38.6 %	46.0 %
10000	30	10	0.01	9.93	95.2 %	113 %	8.93	95.5 %	118 %	0.600	0.00 %	100 %
10000	100	10	0.01	10.0	95.0 %	61.7 %	8.96	91.9 %	63.9 %	0.608	0.00 %	55.7 %
10000	30	100	0.01	100	94.8 %	43.1 %	66.3	4.1 %	54.8 %	70.1	9.8 %	23.0 %

N_E – number of experiments simulated; n_C – number of cultures in each experiment; m – the average number of mutations; ε – plating efficiency. In all simulations, $N_0 = 10^3$ and $N_t = 10^9$. Nominal CI coverage is 95 %. Median CI width was calculated by first expressing the width of CI for each experiment as a percent of the corresponding MLE and then taking the median value.

Fig. 3. Empirical CDFs of mutant counts with different mutant relative fitnesses. One 100,000-tube experiment with $m = 10$ was simulated for each case. For picture clarity, only the values of the CDF up to the colony count of 5000 are shown. Red – $\rho = 1.0$; green – $\rho = 0.8$; blue – $\rho = 1.25$.

3.4. Phenotypic lag

Phenotypic lag, or phenotypic delay, is the time required to express the selectable phenotype by cells that have already acquired mutation in the reporter gene. For example, mutations in *E. coli rpoB* that confer resistance to rifampicin can only be expressed if a sufficient number of wild-type RNA polymerase molecules are replaced by the mutant variants, such that rifampicin does not inhibit transcription to a lethal extent. Disappearance of the wild-type protein can result either from its dilution during cell division, when the daughter cell inherits roughly half of the proteins of the parental cell, or because of protein turnover (degradation and resynthesis). The role of the latter in bacteria depends

on protein half-lives and the doubling time, and for example, in *E. coli* it seems to be small. The doubling time of laboratory *E. coli* strains under optimal conditions can be as short as 20 min [60], while the half-life of RNA polymerase is ~ 200 min [61]. Consequently, Rif[R] phenotypic lag in *E. coli* has been estimated to be 4–5 generations [24]. Therefore, all mutations occurring in the last 4–5 generations will fail to be expressed (in other words, genotypic mutants will not be phenotypic mutants, Fig. 1D). Recently there has been evidence that a big role in phenotypic delay may be played by chromosome segregation in quickly dividing cells [24,62]. Many bacteria in the exponential phase start the next cycle of DNA replication before the previous one is finished, leading to a possibility of a heterozygous state where one copy of a gene of interest acquired mutation, whereas another did not. The target gene copy number may vary depending on its location on the chromosome [63]. If a selectable allele is recessive, it won't be expressed until the cell reaches homozygosity. Simulations performed in the same study suggest that effective polyploidy combined with recessive mutation does not influence mutation rate estimation simply because the increased chance of mutation caused by polyploidy cancels out the phenotypic delay caused by incomplete chromosome segregation [24]. However, effective polyploidy plays a significant role when combined with protein dilution mechanisms [64]. Indeed, since the inhibiting activity of antibiotics requires interaction with their molecular targets, it seems that the significance of protein dynamics in the context of phenotypic lag should not be neglected.

The awareness of the delayed phenotypic expression of a newly acquired allele is widespread in genetic engineering and seemingly less so when reporting fluctuation data, although its effect on mutant distribution has been considered since the model's conception. The possible appearance of phenotypic delay was raised in two big fluctuation experiments reported by Newcombe in 1948 and Boe et al. in 1994 [23, 65]. The phenotypic delay was of interest to Armitage, Crump & Hoel, Koch, Angerer, Stewart et al., and Kissling et al. [5,10,13,16,38,62].

The simplest way to model phenotypic lag, considered by Armitage and further developed by Angerer, is to assume that a certain amount of

Table 2

Analysis of point and interval estimates of m for different values of relative mutant fitness and plating efficiency.

Simulation parameters					MK formulation		LC formulation	
N_E	n_C	m	ε	ρ	median m	CI coverage	median m	CI coverage
10000	30	10	0.8	1.2	10.1	95.3 %	12.0	65.1 %
10000	30	10	0.8	0.8	10.0	95.2 %	8.40	62.8 %
10000	30	10	0.8	0.5	10.0	95.0 %	6.41	0.04 %
10000	30	10	0.5	1.2	10.1	94.6 %	12.0	65.6 %
10000	30	10	0.5	0.8	10.0	94.8 %	8.32	62.9 %
10000	30	10	0.5	0.5	10.0	94.6 %	6.24	0.04 %
10000	30	10	0.1	1.2	10.0	95.0 %	12.6	64.7 %
10000	30	10	0.1	0.8	10.0	94.3 %	7.84	63.4 %
10000	30	10	0.1	0.5	9.99	95.0 %	5.37	0.32 %

N_E – number of experiments simulated; n_C – number of cultures in each experiment; m – the average number of mutations; ε – plating efficiency; ρ – relative mutant fitness. MK formulation – mutant distribution with correction for ρ. LC formulation – simple model where $\rho = 1$. In all simulations, $N_0 = 10^3$ and $N_t = 10^9$. Nominal CI coverage is 95 %.

time (say, t_{lag}) since mutational event must pass for the cell to be able to express mutant phenotype [38]. This time can be imputed as the number of generations (with one generation being the time required for a population to double in size) because, ultimately, it is implicitly expressed by the size of the culture at time $t - t_{lag}$, which we shall denote as N_{lag}. (We remember that t is the time when culture growth is interrupted, that is when $N = N_t$; see (1)).

If mutations occurring after $t - t_{lag}$ are not expressed, the outcome is the same as if no mutations occurred between $t - t_{lag}$ and t (although existing mutants continue proliferating in that time). What this means in practice is that the upper limit of integrals in (6) and (12) becomes $t - t_{lag}$. The formula derived by Angerer (modified to be applicable to the problem at hand) is

$$\left.\begin{aligned} h_0(\Lambda) &= -\frac{1}{\Lambda} \\ h_n(\Lambda) &= \frac{1 - \left(1 - \frac{1}{\Lambda}\right)^n \left(1 + \frac{n}{\Lambda}\right)}{n(n+1)} \text{ for } n \geq 1 \end{aligned}\right\}, \quad (17)$$

where $\Lambda = N_t / N_{lag} = 2^l$. Here l denotes the extent of phenotypic lag in generations. Additionally, it is shown in Supplementary File S1 that when $\varepsilon \neq 1$, the extension of (17) becomes

$$\left.\begin{aligned} h_0(\Lambda, \varepsilon) &= q_0(\Lambda, \varepsilon) \\ h_1(\Lambda, \varepsilon) &= -\zeta q_0 + q_1(\Lambda, \varepsilon) \\ h_n(\Lambda, \varepsilon) &= -\zeta h_{n-1}(\Lambda, \varepsilon) + q_n(\Lambda, \varepsilon) \text{ for } n \geq 2 \end{aligned}\right\}, \quad (18)$$

with

$$\left.\begin{aligned} q_0(\Lambda, \varepsilon) &= \zeta \log\left(\frac{-\varepsilon\Lambda}{s-1}\right) \\ q_1(\Lambda, \varepsilon) &= \zeta\left[\frac{1}{s-1} - \log\left(\frac{-\varepsilon\Lambda}{s-1}\right)\right] \\ q_n(\Lambda, \varepsilon) &= \frac{\zeta}{n(n-1)}\left[1 - \frac{s^{n-1}(s-n)}{(s-1)^n}\right] \text{ for } n \geq 2 \end{aligned}\right\}, \quad (19)$$

and $s = \varepsilon(1 - \Lambda)$.

In the Lea–Coulson model, the lifetimes of individual mutant cells are independent and exponentially distributed random variables. From this angle, the constant (in terms of time) phenotypic lag seems overly severe: some cells may acquire mutation during the lag time but undergo enough divisions such that sensitive protein will be sufficiently diluted. Naturally, the impact will be more significant with longer phenotypic lag and a lower mutation rate. To include an element of stochasticity to the Angerer model, we might assume that the lengths of phenotypic lag l of every mutant clone are i.i.d. random variables obeying the Poisson distribution with some mean λ. The new expressions that substitute (17) and (19), respectively, assume the forms:

$$\left.\begin{aligned} h_0(\lambda) &= -\frac{e^{-\lambda}}{2} \\ h_n(\lambda) &= \sum_{l=0}^{\infty} \frac{e^{-\lambda}\lambda^l}{l!} \frac{1 - \left(1 - \frac{1}{\Lambda}\right)^n\left(1 + \frac{n}{\Lambda}\right)}{n(n+1)} \text{ for } n \geq 1 \end{aligned}\right\}, \quad (20)$$

$$\left.\begin{aligned} q_0(\lambda, \varepsilon) &= \sum_{l=0}^{\infty} \frac{e^{-\lambda}\lambda^l}{l!} \zeta \log\left(\frac{-\varepsilon l}{s-1}\right) \\ q_1(\lambda, \varepsilon) &= \sum_{l=0}^{\infty} \frac{e^{-\lambda}\lambda^l}{l!} \zeta\left[\frac{1}{s-1} - \log\left(\frac{-\varepsilon\Lambda}{s-1}\right)\right] \\ q_n(\lambda, \varepsilon) &= \sum_{l=0}^{\infty} \frac{e^{-\lambda}\lambda^l}{l!} \frac{\zeta}{n(n-1)}\left[1 - \frac{s^{n-1}(s-n)}{(s-1)^n}\right] \text{ for } n \geq 2 \end{aligned}\right\}, \quad (21)$$

with Λ and s appropriately substituted.

Delayed phenotypic expression of a mutant phenotype has the biggest

impact on the lower tail of the mutant distribution [5,13,36], which is reflected in the shapes of the empirical cumulative distribution functions (CDFs) in Fig. 4. Accordingly, Table 3 shows that the phenotypic lag of just two generations decreases mutation rate estimates by almost half.

To test the performance of the novel stochastic Angerer model against real-world data, two famous experiments performed by Newcombe [23] and by Boe et al. [65] were revisited. The Newcombe study reported eight 25-tube (200 μl each) experiments. Each culture was inoculated with either 10^1 or 10^3 cells and grown to an average of 3.5×10^8 cells (see Table 1 in the original paper). Newcombe used two methods to calculate m and observed that the P^0 method gave a much lower estimate than Luria–Delbrück's method of the mean. Ruling out the possibility of an upward bias, he suspected that the discrepancy might result from the phenotypic delay, which affects mainly the distribution's lower tail. Since the P^0 method uses the proportion of cultures containing 0 mutants, it is the most sensitive to bias caused by phenotypic lag.

Several methods of accounting for phenotypic lag have been proposed. One is to discard the lower tail of the empirical CDF and fit the rest [13]. Koch proposed another: he suggested dividing colony counts by 2^l to see the mutant distribution as it was before phenotypic lag started [36]. Newcombe also presented methods based on the mean number of cells in each culture [23].

Recently, the CDF and the Koch methods were employed, using minimization of the sum of squared errors, to jointly find the value of m and the size of the phenotypic lag in the Newcombe experiment [51]. The extent of phenotypic delay has been estimated at 3–4 generations, in agreement with analysis by Armitage [13], and the adjusted mutation rate between 1.34×10^{-8} and 2.82×10^{-8}.

Here I will employ maximum likelihood estimation under Lea–Coulson and stochastic Angerer models to find the possible values of m and λ. The MLEs of μ under the Lea–Coulson formulation range from 4.27×10^{-9} to 1.13×10^{-8}. For all experiments combined, the $\hat{\mu}$(with the hat atop a symbol denoting its maximum likelihood estimate) is 6.88×10^{-9} (95 % CI, $5.99-7.84 \times 10^{-9}$). Joint estimation produces $\hat{\mu}$ of 7.84×10^{-9} to 5.27×10^{-8} and $\hat{\lambda}$ between 0.856 and 4.77. When all data are combined, one obtains $\hat{\mu} = 2.45 \times 10^{-8}$ (95 % CI, $1.76-3.46 \times 10^{-8}$) and $\hat{\lambda}$ 3.17 (95 % CI, 2.44–3.94). The estimates are, therefore, in good agreement with previous analyses.

A similar investigation was performed using data reported by Boe et al. [65]. Twenty-three experiments, each comprising 48 parallel tubes, were performed. Cultures were inoculated with a varying number
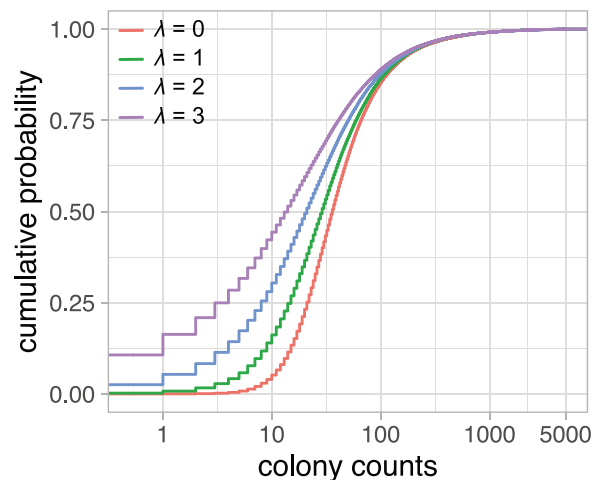

Fig. 4. Empirical CDFs of mutant counts with phenotypic lag constant within a clone, but Poisson-distributed from clone to clone. One 100,000-tube experiment with $m = 10$ was simulated for each case. For picture clarity, only the values of the CDF up to the colony count of 5000 are shown. Red – $\lambda = 0$; green – $\lambda = 1$; blue – $\lambda = 2$; purple – $\lambda = 3$.

Table 3

Analysis of point and interval estimates of *m* for different extents of phenotypic lag and plating efficiencies.

Simulation parameters					SA formulation		LC formulation	
N_E	n_C	m	ε	λ	median m	CI coverage	median m	CI coverage
10000	30	10	1	1	10.0	95.1 %	7.66	35.3 %
10000	30	10	1	2	10.0	94.8 %	5.41	1.32 %
10000	30	10	1	3	10.1	94.9 %	3.48	0.020 %
10000	30	10	0.5	1	10.0	95.2 %	7.80	44.7 %
10000	30	10	0.5	2	10.1	94.9 %	5.66	3.02 %
10000	30	10	0.5	3	10.1	95.3 %	3.80	0.020 %
10000	30	10	0.1	1	10.0	94.7 %	8.16	71.6 %
10000	30	10	0.1	2	10.0	94.9 %	6.35	23.5 %
10000	30	10	0.1	3	9.98	94.5 %	4.66	2.67 %

N_E – number of experiments simulated; n_C – number of cultures in each experiment; m – the average number of mutations; ε – plating efficiency; λ – average phenotypic lag. In all simulations, $N_0 = 10^3$ and $N_t = 10^9$. SA formulation – stochastic Angerer formulation; mutant distribution with correction for λ. LC formulation – simple model where $\lambda = 0$. Nominal CI coverage is 95 %.

(order of magnitude 10^1-10^4) of cells, but this parameter was deemed of little importance. The final size of the culture is not provided in the paper; thus, I will focus on the estimates of *m*. Under the Lea–Coulson model, $\hat{m} = 0.737$ (95 % CI, $0.679-0.797$), whereas under the stochastic Angerer model, it is $\hat{m} = 0.954$ (95 % CI, $0.805-1.136$), and the estimate of phenotypic lag is $\hat{\lambda} = 0.601$ (95 % CI, $0.259-0.957$). Similar results were obtained in the analysis using historical methods (the estimates of phenotypic lag were between 0.6 and 1) [51].

Barna [51] also performed two experiments with *E. coli* cells growing in a defined medium containing glucose or maltose as a carbon source. This change affects the population doubling time (from ~ 23 to ~ 48 min, respectively), but also the estimates of mutation rate under the Lea–Coulson model: $\hat{\mu} = 6.99 \times 10^{-7}$ (95 % CI, $4.60 \times 10^{-7}-1.00 \times 10^{-6}$) in case of glucose medium and $\hat{\mu} = 2.02 \times 10^{-6}$ (95 % CI, $1.58-2.52 \times 10^{-6}$) in case of maltose medium. The 3.5-fold difference has been ascribed to phenotypic lag, estimated to be between 1.58 and 2 generations. Joint estimation of *m* and λ shows significant differences only with glucose data with the new mutation rate of $\hat{\mu} = 1.59 \times 10^{-6}$ (95 % CI, $0.64-4.33 \times 10^{-6}$) and phenotypic lag of $\hat{\lambda} = 1.71$ (95 % CI, $0.03-3.63$) generations. The difference between glucose and maltose data is insignificant when one accounts for the phenotypic delay. To conclude, the stochastic Angerer model reiterates the results obtained using historical methods.

Considering recent evidence for the significance of protein dilution for the expression of a mutant phenotype in bacteria, it is worth investigating how the above model with stochastic phenotypic lag performs against data simulated with consideration for protein dilution. The simulation algorithm is based on the one from Barna [51]. It takes two arguments: the initial number of wild-type proteins *u* in the cell and some threshold value of the number of wild-type proteins in the cell, smaller than *u*, above which the said cell is sensitive to the antibiotic. As argued in [64] (see Supplemental Information in the referenced paper), with *u* protein units initially in the cell, resistance emerges approximately after $\lambda = \log_2 u$ generations (see equation S1 in [64]); therefore, we have simulated 1, 2, 3, or 5 generations of phenotypic lag by setting *u* to 2, 4, 8, or 32, respectively (Table 4). However, this is only a mean estimate of when a randomly chosen cell should develop resistance, and it does not consider the whole population, in which wild-type protein levels in all cells are co-dependent. Additionally, in a scenario where wild-type proteins are entirely distributed into daughter cells, *u* cells possess a single unit of the wild-type protein. These cells can never reach phenotypic resistance if one assumes that the wild-type proteins must be diluted entirely out of the cell for it to lose sensitivity. Therefore, to allow for the whole mutant clone to become resistant, in the simulations, the threshold value was set to 1. Since the protein dilution model is indexed by more parameters than the stochastic Angerer model, one can anticipate that *u* might not easily translate into λ; thus, *m* and λ were estimated jointly. The stochastic Angerer model approximates protein dilution with acceptable precision and accuracy: the error of the point estimation of *m* as judged by the median, is not bigger than ~ 5–10 % of the true value, and the confidence intervals retain coverage close to nominal in all cases except when both sample size and phenotypic lag are small ($n_C = 30$, $u = 2$) (Table 4). This, however, is not caused by the

Table 4

Assessment of efficiency of stochastic Angerer formulation of the Luria–Delbrück distribution against protein dilution model.

Simulation parameters				Joint estimation			LC formulation		Observed power
N_E	n_C	m	u	median m	CI coverage	median λ	median m	CI coverage	
10000	100	1	2	1.06	95.1 %	0.938	0.703	24.6 %	50.6 %
10000	100	1	4	1.10	94.6 %	1.75	0.502	0.43 %	85.2 %
10000	100	1	8	1.10	95.0 %	2.42	0.354	0.0 %	93.5 %
10000	100	1	32	0.97	94.9 %	3.46	0.179	0.0 %	92.8 %
10000	100	10	2	9.96	95.3 %	0.739	8.20	13.4 %	46.4 %
10000	100	10	4	10.1	94.6 %	1.49	6.60	0.06 %	91.5 %
10000	100	10	8	10.3	94.9 %	2.22	5.07	0.0 %	99.8 %
10000	100	10	32	9.86	94.7 %	3.49	2.60	0.0 %	100 %
10000	30	1	2	1.06	96.8 %	0.900	0.699	67.0 %	20.9 %
10000	30	1	4	1.11	95.5 %	1.72	0.500	25.8 %	42.1 %
10000	30	1	8	1.08	95.7 %	2.38	0.353	5.2 %	52.6 %
10000	30	1	32	0.95	95.6 %	3.40	0.183	0.0 %	54.3 %
10000	30	10	2	9.78	96.6 %	0.592	8.23	55.3 %	18.6 %
10000	30	10	4	9.82	95.1 %	1.35	6.66	11.5 %	47.5 %
10000	30	10	8	10.0	95.1 %	2.12	5.11	0.78 %	77.3 %
10000	30	10	32	9.64	94.7 %	3.39	2.61	0.0 %	97.0 %

The threshold value of protein units in the cell above which the phenotype is not expressed has been set to 1. N_E – number of experiments simulated; n_C – number of cultures in each experiment; m – the average number of mutations; u – initial number of protein units; λ – average phenotypic lag. In all simulations, $N_0 = 10^3$ and $N_t = 10^9$. Joint estimation – MLEs of *m* and λ were estimated simultaneously under the stochastic Angerer model. LC formulation – estimation of *m* under the Lea–Coulson formulation. Nominal CI coverage is 95 %. Observed power – percent of estimations with λ significantly ($P < 0.05$) greater than 0.

model itself but rather by the well-known inaccuracy of the likelihood ratio test near the boundary of the parameter space: the confidence intervals for m cannot be correctly estimated if the value of the nuisance parameter λ reaches 0, which is the minimum value λ can assume, and which violates the regularity conditions of Wilks' theorem [66] (in agreement with that, λ was found to be significantly greater than 0 only in ~ 20 % cases, Table 4). However, the good CI coverage when regularity conditions are met might be related to the fact that the shapes of the CDFs under the protein dilution model and under the stochastic Angerer model with m and λ chosen to be the same as joint estimates from protein dilution simulated data are remarkably similar (Fig. 5).

When the threshold value in the stimulations is set to 0, the stochastic Angerer model performs somewhat worse, albeit better than expected, with the median m being lower than the nominal value by about 10 % in the case of 2–8 protein units and by ~ 30 % in case of 32 protein units, and CI coverage around 90 % not only for a more realistic sample size ($n_C = 30$) but also for a larger one ($n_C = 100$) which should be more sensitive to deviations from the model assumptions (Table S1). Based on these results, as well as the good agreement of the estimates with previously published data, the stochastic Angerer model may be helpful when analyzing data affected by phenotypic delay even though it does not exactly reflect the physiological nature of the process, particularly because the exact distribution of the number of resistant bacteria under the protein dilution model (or protein dilution combined with effective polyploidy) is currently unknown.

It should also be noted that there does not seem to be one correct method to model phenotypic delay: in some organisms, such as eukaryotic (particularly mammalian) cells, protein degradation might play a more significant role. For example, the doubling time of *Saccharomyces cerevisiae* is 1.5–2.3 h [67], and the half-lives of protein products of the popular reporter genes such as *URA3* or *CAN1* may vary between 1.4 and 3 h [68,69]. While arguably some form of accounting for the phenotypic delay is better than not correcting at all, it will be interesting to see in the future how a "mechanism-agnostic" formulation such as the one presented above fares against other, more biologically relevant models.

3.5. Cell death

Under the classic Luria–Delbruck model, the population growth is modeled by a pure birth process, where we assume no cell death. However, there are certain scenarios where death events can frequently occur, for example:

- Selectable mutation acquired during growth increases the chance of dying of a mutant cell. Wild-type cells are unaffected. This will introduce a negative bias when estimating the mutation rate.
- The assayed bacterial strain carries certain genetic mutations that severely affect cellular fitness. Both wild-type and mutant cells will be affected.
- Cells grow in the presence of a sub-inhibitory concentration of an antibiotic. Again, wild-type and mutant cells can be subjected to death unless one scores for mutations leading to resistance to the said antibiotic. In such a case, only wild-type cells are sensitive, as selective pressure will lead to the selection of resistant cells.

Several new symbols need to be introduced. In addition to the previously defined β, the growth rate of a strain, the mean death rate is typically denoted by δ. These are assumed to be constant over time.

Further, to ensure population growth, we assume that $\beta > \delta$. We can express death rate as a fraction of growth rate $\delta = d\beta$. Additionally, we can express the death of a cell in terms of probability. The probability of cell death is $p = d/(1 + d)$, implying that $d = p/(1 - p)$. Since we assumed $d < 1$, $p < 0.5$.

We can extend the assumption of deterministic growth of non––mutant cells by saying that these cells *grow and die* deterministically, which means that β in (1) and (4) is replaced by the net growth rate $\beta* = \beta - \delta = \beta(1 - d)$. This should hold for reasonable values of d and sufficiently large inocula. For example, under a simple stochastic model, the chance of extinction as $t \longrightarrow \infty$ of a population starting with N_0 cells is d^{N_0} (see (8.59) in [15]), so for example, for $d = 0.9$ and $N_0 = 1000$, the chance of extinction is $\sim 10^{-46}$. The impact of the stochastic growth of non-mutant cells on the estimates of mutation rates will be discussed in the next section.

It is important to remember that in the described model, cells mutate during division (hence the name mutation rate per cell division). Thus expressions (1) to (4) are of use only when the number of divisions can be equated to $N_t - N_0$. This is not the case when there is cell death, as in this scenario, some divisions are masked by dying cells. When cell death occurs, more divisions are required to reach the same number of cells (Fig. 1F). The real number of cell divisions can be extracted by simple reasoning. If the chance of death of a wild-type cell is p, out of a given number of wild-type cell events, a fraction p will be deaths, and $1 - p$ will be births; for example, when $p = 0.4$ (which implies $d = 2/3$), out of 10 events we will have 6 births and 4 deaths, so starting from a single ($N_0 = 1$) cell we have $N_t = 1 + 1 + 1 + 1 + 1 + 1 + 1 - 1 - 1 - 1 - 1 = 3$. The increase in cell count is $N_t - N_0 = 2$. On the other hand, $N_t - N_0 =$ Births − Deaths, and Births/Deaths $= (1 - p)/p = 1/d$, so the number of cell divisions is clearly Births $= (N_t - N_0)/(1 - d) = 6$. Hence, when wild-type cell death occurs, mutation rates are inflated by a constant factor $(1 - d)^{-1}$. The correcting factor was first derived by Newcombe [23] and reiterated by Zheng [46]. The phenomenon of overestimation of mutation rates due to cell death was also reported by Frenoy & Bonhoeffer based on similar reasoning supported by simulations [70].

The dynamics of the mutant cells can be modeled by a simple birth-and-death process, as previously suggested [30,37,43,71,72]. Under this model, upon completion of the lifetime, a cell can either divide ($+1$) or die (-1). The most profound difference between mutant and non-mutant cells is that each mutant clone starts with a single cell; therefore, its chance of dying cannot be neglected: if the original mutant cell dies, the whole mutant lineage will never be. Consequently, mutant cell death introduces a downward bias on mutation rate estimation (Fig. 1E).

For reasons explained later, I will focus on the situation where the death rate is the same for wild-type and mutant cells, that is, $\beta_1^*/\beta_2^* = r^* = \beta_1/\beta_2 = r$. Here, β_1^* and β_1^* are the mean per capita growth rates of non-mutants and mutants, respectively. (The case when $d_1 \neq d_2$, for example, when cells are exposed to a sub-inhibitory concentration of an antibiotic and $d_2 = 0$ was studied by Zheng [46]). The expression for the auxiliary sequence $\{h_n\}$ assumes the form

$$\left. \begin{array}{ll} h_0(r, d) = & -1 + rd\mathbf{B}(r; 2)\mathbf{F}(1, r; r + 2; d) \\ h_n(r, d) = & (1 - d)^2 r\mathbf{B}(n; 1 + r) \\ & \mathbf{F}(n + 1, r + 1; n + r + 1; d) \quad \text{for } n \geq 1 \end{array} \right\} . \tag{22}$$

When only a part of the culture is plated, the expression is somewhat more complicated:
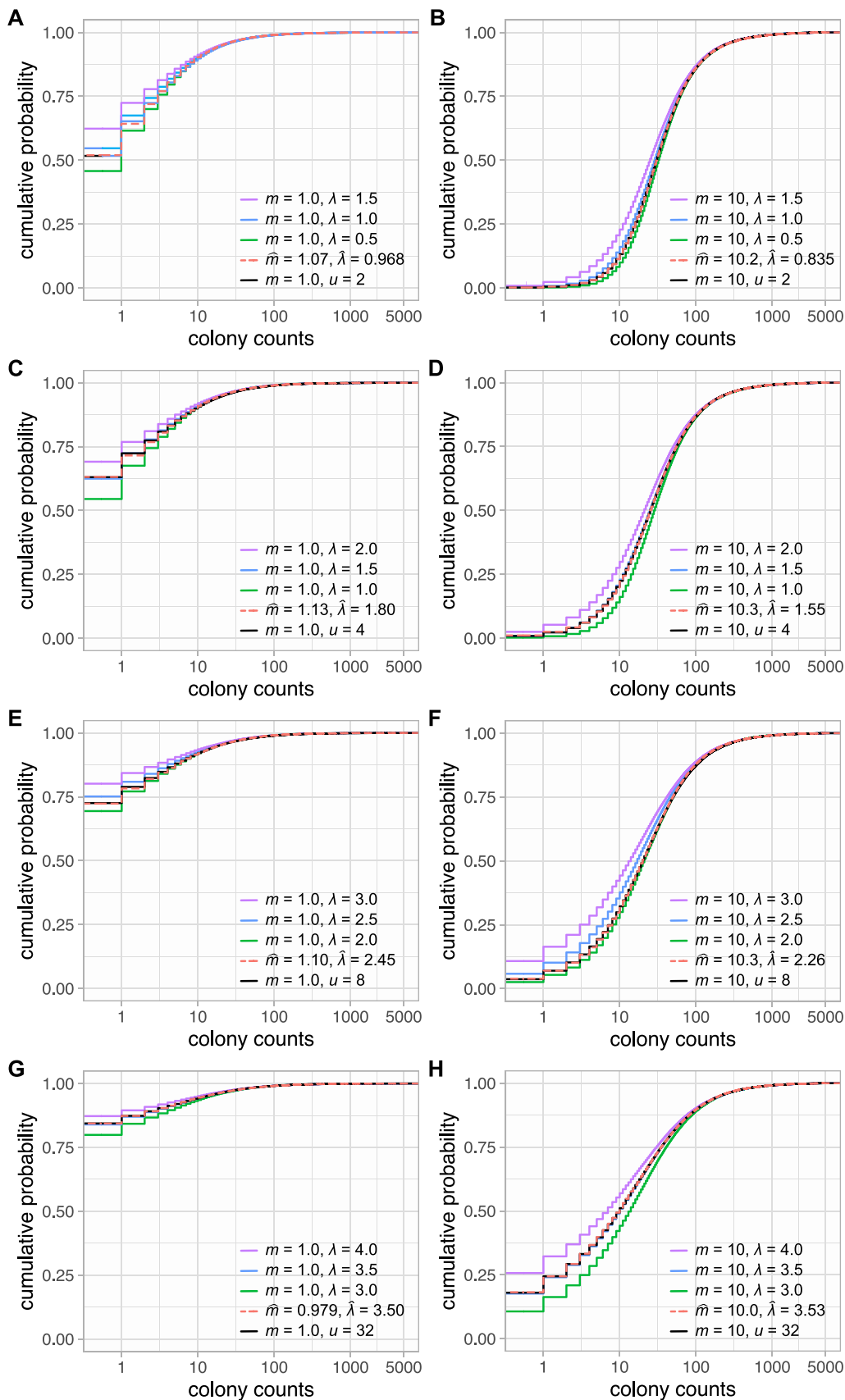
Fig. 5. Empirical CDFs of mutant counts under the protein dilution model. One 100,000-tube experiment with $m = 1$ (A, C, E, G) or $m = 10$ (B, D, F, H), and the initial number of protein units cell $u = 2$ (A, B), $u = 4$ (C, D), $u = 8$ (E, F), or $u = 32$ (G, H) that need to be diluted down to 1 or less for the phenotype to be expressed was simulated for each case. Black continuous lines represent the empirical CDFs. MLEs of m and λ estimated jointly from these data, but assuming stochastic Angerer distribution, were used to simulate additional experiments under the stochastic Angerer model. These CDFs are represented by red dashed lines. Additional CDFs are presented for reference. For picture clarity, only the values of the CDF up to the colony count of 5000 are shown.

$$
\left.
\begin{aligned}
h_0(r,d,\varepsilon) = &\ -1 + rd\mathbf{B}(r;2) + \mathbf{F}(1,r;r+2;d)\frac{1-d}{r+1}[d\mathbf{F}(1,1+r;2+r;d)\\
&+ \frac{(1-\varepsilon-d)}{\varepsilon}
\begin{cases}
\mathbf{F}\left(1,1+r;2+r;\dfrac{\varepsilon+d-1}{\varepsilon}\right) & d_2 > 1-2\varepsilon\\[2ex]
\dfrac{\varepsilon}{1-d}\mathbf{F}\left(1,1;2+r;\dfrac{\varepsilon+d-1}{d-1}\right) & \text{otherwise}
\end{cases}
]\\[2ex]
h_n(r,d,\varepsilon) = &\ \frac{r(1-d)^2}{\varepsilon}\mathbf{B}(n;1+r)\\
&
\begin{cases}
\mathbf{F}\left(n+1,r+1;n+r+1;\dfrac{\varepsilon+d-1}{\varepsilon}\right) & d > 1-2\varepsilon\\[2ex]
\left(\dfrac{\varepsilon}{1-d}\right)^{r+1}\mathbf{F}\left(r+1,r;n+r+1;\dfrac{\varepsilon+d-1}{d-1}\right) & \text{otherwise}
\end{cases}
\quad \text{for } n \geq 1
\end{aligned}
\right\}.
\tag{23}
$$

Simulations show that the upward bias from an increased number of divisions has a dominant effect over the downward bias caused by dying mutant clones, resulting in higher mutant counts (Fig. 6) and over-estimated mutation rates (Table 5). Small death rates (< 10 % of growth rate) have little impact on the point estimates of mutation rates. However, the bias quickly rises; at $d = 0.25$, the difference is ~ 20 %. At $d = 0.6 - 0.7$, mutation rates are essentially doubled (Table 5).

In the end, I would like to discuss the case when the presence of an antibiotic in the liquid medium promotes the selection of resistant bacteria ($d_1 \neq d_2 = 0$), which was studied in [46]. Under the assumptions considered above, bacterial growth in the presence of a sub-inhibitory concentration of an antibiotic has, apart from increasing the number of cell divisions, the additional effect of decreasing the net growth rate of the non-mutant cells, leading to $r < 1$ and thus further inflating mutant counts. However, setting a very big wild-type death rate, such as $d_1 = 0.95$ leads to $r^* = 0.05$. When the wild-type population grows so much slower than the mutant cells, one can quickly encounter a situation where the mutant count is much bigger than that of non-mutants, violating the requirement that mutant cells comprise only a negligible part of the culture. Additionally, the switch to phenotypical resistance is probably not instantaneous. In reality, mutant cells will continue to die at the same rate as wild-type cells for the period of phenotypic lag, or

possibly with a gradual change of death rate from that of wild-type cells to that of mutants (in any case, the mutant death rate is probably not constant over time). As departing from these useful assumptions would inevitably lead to a significantly more complicated model, for the time being, mlemur cannot treat such cases.

3.6. Variation of the final number of cells in parallel cultures

Under the Luria–Delbrück model, we assume that each sister culture contains the same number of cells. It is clear, however, that complete homogeneity of the culture sizes is impossible to achieve. This problem has been studied previously by Ycart and Veziris, and Zheng [41,42,73]. Because the mutation rate is constant, a smaller number of cells in a given culture will result in a smaller average number of mutations (see (3)), increasing the fraction of smaller colony counts. As the Luria–Delbrück distribution's PMF values are generally bigger for smaller colony counts, one can deduce that high variability in culture size will deflate the mutation rate estimate.

A good unitless measure of dispersion is the coefficient of variation (CV), which is the standard deviation (SD) divided by the mean number of cells in each culture (N_t). Two studies were conducted to assess the impact of CV on the estimates of m. In the study by Ycart and Veziris, the fluctuation data were simulated assuming a log-normal, gamma, or other similarly shaped distribution [42]. In Zheng 2016, each culture was simulated using a Bartlett stochastic algorithm [41]. These works concluded that a CV as big as 0.2 has an insignificant impact on the estimates of m.

When CV is big, Zheng proposed two methods to deal with extra variability. One is to use the B^0 distribution, a mixture of gamma and Luria–Delbrück distributions indexed by m and CV [40,41]. While mutant counts are Luria–Delbrück distributed, the parameter m is a random variable obeying the gamma distribution. The CV of m is assumed to be the same as the CV of N_t. Another method is the so-called "Golden Benchmark method", which means estimating μ directly using pairs of mutant counts and population sizes for each test tube [41].

In the current study, I investigated the impact of CV in the context of wild-type cell death. The model developed in the previous section neglects the stochastic nature of the wild-type dynamics, whose important consequence is the inflation of the variance of culture size. If we assume that wild-types grow according to the simple birth and death process, then using (8.48) and (8.49) in [15] and with minor rearrangements, we arrive at the following formula for the coefficient of variation of N_t:

$$
CV = \sqrt{\frac{1+d}{1-d}\frac{N_t - N_0}{N_t N_0}} \approx \sqrt{\frac{1+d}{N_0(1-d)}}
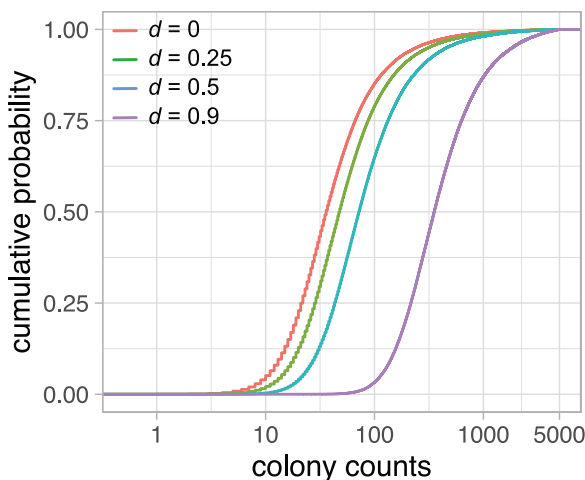\tag{24}
$$

Fig. 6. Empirical CDFs of mutant counts with non-zero death rate. One 100,000-tube experiment with $m = 10$ was simulated for each case. The death rate is the same for wild-type and mutant cells. For picture clarity, only the values of the CDF up to the colony count of 5000 are shown. Red – $d = 0$; green – $d = 0.25$; blue – $d = 0.5$; purple – $d = 0.9$.

Table 5

Analysis of point and interval estimates of *m* under conditions of a non-zero death rate.

Simulation parameters					BD formulation		LC formulation	
N_E	n_C	m	ε	d	median m	CI coverage	median m	CI coverage
10000	30	10	1	0.1	10.0	95.0 %	10.8	89.5 %
10000	30	10	1	0.25	10.0	94.6 %	12.3	53.8 %
10000	30	10	1	0.65	10.1	94.9 %	21.2	0.0 %
10000	30	10	1	0.9	10.0	94.8 %	52.7	0.0 %
10000	30	1	1	0.1	1.00	94.8 %	1.06	93.5 %
10000	30	1	1	0.25	1.00	95.1 %	1.18	87.2 %
10000	30	1	1	0.65	1.00	94.5 %	1.79	19.5 %
10000	30	1	1	0.9	1.00	94.8 %	3.52	0.0 %
10000	30	10	0.1	0.1	10.0	94.8 %	10.8	91.9 %
10000	30	10	0.1	0.25	10.0	94.7 %	12.4	67.2 %
10000	30	10	0.1	0.65	10.1	94.6 %	22.0	0.0 %
10000	30	10	0.1	0.9	10.1	95.0 %	56.0	0.0 %

N_E – number of experiments simulated; n_C – number of cultures in each experiment; *m* – the average number of mutations; ε – plating efficiency; *d* – relative death rate. In all simulations, $N_0 = 10^3$ and $N_t = 10^9$. BD formulation – the Luria–Delbrück model with mutant dynamics modeled using simple birth-death process. LC formulation – the simple model where $d = 0$. Nominal CI coverage is 95 %.

which shows that the coefficient of variation increases with smaller N_0 and bigger *d*. However, setting for example $N_0 = 10^3$, $N_t = 10^8$, and $d = 0.7$ gives $CV = 0.075$. Even *d* as big as 0.95 gives $CV = 0.197$, within the 20 % safety threshold [41], indicating that the variability might be controlled so long as the inoculum is sufficiently big.

To test whether one can model the dynamics of the wild-types using a deterministic approach with acceptable results, I simulated fluctuation data using the fully stochastic fixed-time Bartlett algorithm by Qi Zheng, which can be found in the rSalvador source files and was described in [46]. The fate of the culture is tracked event by event, and each event might be one of four: wild-type birth, wild-type death, mutant birth, or mutant death, with mutant birth resulting from either cell division or mutation. The lifetimes of all cells are exponentially distributed. Consequently, the number of births and deaths, their ratio, and N_t are all random variables (because the process is stochastic). However, with a sufficiently long growth time, the mean number of births should be close to its deterministic equivalent, which, as shown previously, is given by $(N_t - N_0)/(1 - d)$. For example, if one sets $N_0 = 100$, $t = 15.4$, $\mu = 10^{-4}$,

and $d = 0.7$ (which corresponds to $\beta_1 = 1, \beta_2 = 1, \delta_1 = 0.7, \delta_2 = 0.7$ in the simulation algorithm), the average N_t from 10^6 simulated test tubes is 10,086, and the mean number of births is 33,287. The same number of births is produced in the deterministic setting as calculated using $(10\,086 - 100)/(1 - 0.7)$.

I have simulated a series of 10,000 100-tube experiments with the values of *d* between 0.5 and 0.9, $\mu = 10^{-4}$ or 10^{-5}, and *t* chosen such that N_t varied from 10^4 to 2.5×10^5 (which corresponded to *m* between 1 and 25). Since N_t was kept relatively small to save computational time, and in some cases, φ was as big as 0.02, I chose to correct for the size of the inoculum in the estimations of *m*. However, in a real-world scenario, the number of wild-type cells is unknown because the number of colonies on non-selective plates is a sum of mutant (*n*) and non-mutant colonies (N_t). Therefore, μ was estimated using the average total culture size: to obtain the estimate, *m* was divided by $(N_t + n - N_0)/(1 - d)$.

The experiments demonstrate that when the number of wild-types is a random variable (because of their stochastic growth), μ is slightly

Table 6

Point and interval estimates of μ under a fully stochastic model with cell death.

	Simulation parameters							Culture size		LD distribution		B^0 distribution		Golden Benchmark	
Line	N_E	n_C	N_0	t	$10^4\mu$	d	ρ	10^{-4} median $N_t + n$	median CV	10^4 median μ	CI coverage	10^4 median μ	CI coverage	10^4 median μ	CI coverage
1	10000	100	100	9.2	1	0.5	1	0.996	17.2 %	0.987	95.4 %	1.00	95.6 %	0.999	95.3 %
2	10000	100	100	12.4	1	0.5	1	4.93	17.2 %	0.976	93.3 %	1.00	95.7 %	1.00	95.1 %
3	10000	100	100	13.8	1	0.5	1	9.94	17.2 %	0.969	90.4 %	1.00	95.9 %	1.00	94.9 %
4	10000	100	200	12.4	1	0.5	1	9.87	12.2 %	0.985	93.6 %	1.00	95.7 %	1.00	95.1 %
5	10000	100	100	15.4	1	0.7	1	1.02	23.6 %	0.975	94.9 %	1.00	96.1 %	1.00	95.6 %
6	10000	100	100	20.7	1	0.7	1	4.99	23.7 %	0.950	86.7 %	1.00	96.0 %	1.00	94.9 %
7	10000	100	100	20.7	1	0.7	0.8	4.98	23.7 %	0.953	86.4 %	1.00	96.2 %	1.00	94.8 %
8	10000	100	100	23	1	0.7	1	9.95	23.7 %	0.938	77.4 %	0.999	96.4 %	1.00	94.9 %
9	10000	100	100	23	0.1	0.7	1	9.92	23.7 %	0.971	94.7 %	0.998	95.9 %	0.999	95.2 %
10	10000	100	250	17.7	1	0.7	1	5.07	15.0 %	0.981	93.5 %	1.00	95.6 %	1.00	94.8 %
11	10000	100	250	20	1	0.7	1	10.1	15.0 %	0.975	92.0 %	1.00	95.5 %	1.00	95.0 %
12	10000	100	500	17.7	1	0.7	1	10.1	10.6 %	0.988	93.8 %	1.00	95.2 %	1.00	95.0 %
13	10000	100	250	53	1	0.9	1	5.04	27.3 %	0.926	75.7 %	1.00	96.6 %	1.00	94.8 %
14	10000	100	500	46.1	1	0.9	1	5.05	19.3 %	0.964	89.9 %	1.00	95.9 %	0.999	95.0 %
15	10000	100	500	53	1	0.9	1	10.1	19.4 %	0.956	85.1 %	0.999	96.1 %	0.999	95.4 %
16	10000	100	500	53	0.1	0.9	1	10.1	19.4 %	0.978	94.5 %	0.100	95.4 %	0.100	95.0 %
17	10000	100	1000	46.1	1	0.9	1	10.1	13.7 %	0.979	92.3 %	1.00	95.5 %	0.999	94.7 %
18	10000	100	1000	55.2	1	0.9	1	25.1	13.7 %	0.974	89.2 %	0.999	96.0 %	0.998	95.1 %
19	10000	100	2000	39.1	1	0.9	1	10.0	9.6 %	0.989	94.5 %	0.999	95.7 %	0.999	95.4 %

N_E – number of experiments simulated; n_C – number of cultures in each experiment; N_0 – the size of inoculum; *t* – time of culture growth; μ – mutation rate per cell; *d* – relative death rate; ρ – relative mutant fitness; $N_t + n$ – the average final number of cells in the culture (non-mutant and mutant). Cell cultures were simulated using a fully stochastic Bartlett algorithm until a prescribed value of $N_t + n$ was reached but modeled by a simple birth-death process for mutants with deterministic growth of wild-types, with consideration for the inoculum, using either Luria–Delbrück distribution or B^0 distribution where *CV* is taken into account. For each experiment, μ was calculated by dividing the estimate of *m* by $(N_t + n - N_0)/(1 - d)$. Mean and *CV* for N_t were calculated for each experiment, and the median values are presented in the table. Nominal CI coverage is 95 %.

underestimated when one uses the Luria–Delbrück distribution with cell death, as judged by the median μ lower by 1–7 % than the nominal value. The results show that the performance of both point and interval estimates strongly depends on the size of the inoculum, as this parameter significantly affects CV, but also on N_t, or rather on the associated m (Table 6, column LD distribution). For example, for $d = 0.7$, $\mu = 10^{-4}$, and $N_0 = 100$, the 95 % CI coverage when $N_t \approx 10^4$ ($m \approx 1$) is 94.9 %, but when $N_t \approx 5 \times 10^4$ ($m \approx 5$), it is 86.7 % and for $N_t \approx 10^5$ ($m \approx 10$) it drops to 77.4 %, even though in all these cases CV remains stably around 24 % (Table 6, lines 5–8). The likely explanation for this observation is that bigger values of m produce higher per-plate mutant counts, increasing precision, and this, in turn, negatively affects CI coverage; for example, decreasing mutation rate to 10^{-5} while keeping $N_t \approx 10^5$ ($m \approx 1$) increases CI coverage to 94.7 % (Table 6, compare lines 8 & 9). The drop in accuracy might be alleviated by decreasing the variability in culture sizes: for $\mu = 10^{-4}$ and $N_t \approx 10^5$ ($m \approx 10$), increasing N_0 to 250 ($CV \approx 15$ %) gives 95 % CI coverage 92.0 %, and for $N_0 = 500$ ($CV \approx 11$ %) it is 93.8 % (Table 6, compare line 8 to lines 11–12). Similar observations can be made for the case where $N_t \approx 5 \times 10^4$ ($m \approx 5$) (Table 6, compare lines 6 & 10).

The usage of B^0 distribution significantly improves the accuracy of point estimates of μ at any value of CV, albeit at the cost of producing too conservative confidence intervals when CV or m is high (one can observe 95 % CI coverage at 95.2–96.6 %, Table 6, column B^0 distribution). This problem only affects the CIs of μ, and the confidence intervals of m retain the correct coverage; for example, if, in the estimations described in Line 8 of Table 6 we replace each observed N_t with the mean from 10^6 test tubes (pooled from all experiments) equal 9.95×10^4, the CI coverage becomes 95.0 %. The cause of this discrepancy is that it is the value of m that is directly estimated by the algorithm, and the variability in N_t is reflected in a similar variability in m, which is already incorporated in the model. Dividing m by the true value of N_t results in a situation where we correct for the variability in culture sizes twice. Consequently, values of m farther from the true value are partially offset by similar variability of N_t. Thus, the observed variance of μ is smaller than anticipated, and the CI coverage increases.

Alternatively, if the values of N_t for each culture are known, one can also use the Golden Benchmark method described in previous paragraphs: one may note a high accuracy of point estimates and CI coverage at 94.7–95.6 % (Table 6, column Golden Benchmark). The good performance of the Golden Benchmark method is particularly striking, considering that we disregarded the variability in the proportion of deaths vs. births, replacing it with its mean value equal d. This parameter plays a crucial role in recovering the number of cell divisions from the number of living cells. However, a brief analysis of the number of births and deaths in the simulated data shows that the distribution of the deaths-to-births ratio is characterized by a low variance, which might explain why this parameter seems to have a negligible impact on the estimates in practice (Table S2, Figure S1).

These observations remain consistent when $d = 0.5$ or $d = 0.9$. However, in the latter case, one needs to use bigger inocula (order of magnitude 10^3) to counterbalance the extra variability caused by the high death rate and its effect on the estimates using the Luria–Delbrück distribution (Table 6). Decreasing the sample from 100 to a more realistic 30 cultures per experiment improved the coverage of confidence intervals produced using Luria–Delbrück distribution, which is most evident when one compares, for example, Lines 6, 7, 8, 13, and 15 between Table 6 and Table S3. Overall, these results suggest that it is possible to neglect the stochastic nature of the wild-type cell dynamics without much loss of accuracy and precision of the estimation so long as the values of m and CV are controlled, and cultures are grown for a sufficiently long time.

3.7. A universal sequence?

Feeling encouraged by the number of developments concerning the relaxation of the Luria–Delbrück protocol requirements, it might be appealing to attempt deriving a universal sequence that combines existing generalizations of the Lea–Coulson model. However, one quickly arrives at complex dilemmas, one of which has been described in section 3.6. A related problem can be easily imagined if a researcher wishes to correct simultaneously for differential growth of mutant and wild-type cells and phenotypic lag. If a genetic mutant does not express a resistant phenotype for some time, we can imagine that the same trait will be extended to other phenotypes: growth rate and death rate. In the most naïve scenario, a living cell will instantly change its growth dynamics from that of a wild-type cell to that of a mutant when the period of phenotypic lag expires. While a closed-form expression for the case $d = 0$ can be derived under this assumption, it becomes significantly more complicated when we replace the Yule process with the simple birth-and-death process. Additionally, it seems more realistic that the growth rate and death rate change would be gradual over the period of phenotypic delay as wild-type proteins are being successively replaced by their mutant forms. Instead of taking β and δ as constants, we could model mutant dynamics using a non-homogeneous process such as the one described in chapter 9.3 in Bailey [15]. This, however, raises a question of how exactly the change in β and δ over time occurs.

The outcome of a fluctuation assay may be affected by more than one factor simultaneously. Thus, the statistical model should include as many factors as possible. Alas, the progress in this area is limited by the need for more biological data, the increasing complexity of the model, and the mathematical and computational difficulties associated with it. Hence, the adjustment for the phenotypic lag is currently limited to cases where it is assumed that apart from acquiring the ability to grow on a selective medium, there are no other changes in phenotype (i.e., $\beta_1 = \beta_2$ and $\delta_1 = \delta_2$).

4. Concluding remarks

Eighty years after the publication of the Luria & Delbrück paper, fluctuation analysis has seen numerous developments that aim to relax its strict requirements. For a long time, however, the researchers were limited to a basic protocol that did not account for inter-strain differences in fitness, phenotypic lag, cellular death rate, and other deviations that affect the number of mutant colonies on the plate. One such deviation is imperfect plating, which should be adequately modeled to obtain correct results (Table 1). To this day, the nuances are frequently disregarded, perhaps due to a lack of knowledge, judging by the unfailing popularity of FALCOR (e.g., [74–76]). With the computational power of modern CPUs, it is becoming feasible to incorporate multiple additional parameters to increase the accuracy of mutation rate estimation. The current study provides important extensions to the fluctuation data analysis using the maximum likelihood method, with the possibility to account for cell death or phenotypic lag, particularly with partial plating. The new package mlemur does so in a user-friendly way, allowing one to obtain point and interval estimates and compare them between different strains and for many strains simultaneously. Tools to calculate the statistical power of the likelihood ratio test and to determine the sample size required to achieve the prescribed power have also been implemented in mlemur. These developments have been described in Supplementary File S1, and Table S4 contains an analysis of the required sample sizes for a wide variety of the values of m, which might be valuable when designing a fluctuation experiment.

Nevertheless, the difficulties encountered when modeling bacterial growth in the presence of a sub-inhibitory concentration of an antibiotic underline the fact that the classical Luria–Delbrück distribution, even with extensions, might not be a suitable model for every fluctuation assay. Novel approaches were proposed and might be available for the user in the future [43,44,46,77–80]. The mechanism of phenotypic lag and its impact on growth and death rate is also poorly studied, yet it has a profound effect on the distribution of mutant cells. While the same problems do not plague modern methods based on whole genome

sequencing, the low cost and complexity, and the speed of generating data remain important advantages of the fluctuation assays, warranting further development of more sophisticated statistical models of mutation and cell proliferation.

Funding

Declaration of Competing Interest

The author declares no conflict of interest.

Data availability

The R package mlemur is available at https://github.com/krystianll/mlemur. The R and C++ code for all simulating experiments, simulated fluctuation data, and the results of estimations are available at Zenodo (10.5281/zenodo.7505829).

Acknowledgements

Appendix A. Supporting information

Supplementary data associated with this article can be found in the online version at doi:10.1016/j.mrfmmm.2023.111816.

References

[1] P.L. Foster, Adaptive mutation: implications for evolution, BioEssays 22 (12) (2000) 1067–1074, https://doi.org/10.1002/1521-1878(200012)22:12<1067::AID-BIES4>3.0.CO;2-Q.

[2] P.L. Foster, Stress-induced mutagenesis in bacteria, Crit. Rev. Biochem. Mol. Biol. 42 (5) (2007) 373–397, https://doi.org/10.1080/10409230701648494.

[3] P.L. Foster, H. Lee, E. Popodi, J.P. Townes, H. Tang, Determinants of spontaneous mutation in the bacterium *Escherichia coli* as revealed by whole-genome sequencing, Proc. Natl. Acad. Sci. 112 (44) (2015) E5990–E5999, https://doi.org/10.1073/pnas.1512136112.

[4] E. Shor, J. Schuyler, D.S. Perlin, A novel, drug resistance-independent, fluorescence-based approach to measure mutation rates in microbial pathogens, mBio 10 (1) (2019) 1–13, https://doi.org/10.1128/mBio.00120-19.

[5] W.A. Rosche, P.L. Foster, Determining mutation rates in bacterial populations, Methods 20 (1) (2000) 4–17, https://doi.org/10.1006/meth.1999.0901.

[6] S.E. Luria, M. Delbrück, Mutations of bacteria from virus sensitivity to virus resistance, Genetics 28 (6) (1943) 491–511, https://doi.org/10.1002/14651858.CD011168.

[7] D.E. Lea, C.A. Coulson, The distribution of the numbers of mutants in bacterial populations, J. Genet. 49 (3) (1949) 264–285, https://doi.org/10.1007/BF02986080.

[8] Q. Zheng, A cautionary note on the mutation frequency in microbial research, Mutat. Res. - Fundam. Mol. Mech. Mutagen. 809 (February) (2018) 51–55, https://doi.org/10.1016/j.mrfmmm.2018.04.001.

[9] A. Couce, J. Blázquez, Estimating mutation rates in low-replication experiments, Mutat. Res. - Fundam. Mol. Mech. Mutagen. 714 (1–2) (2011) 26–32, https://doi.org/10.1016/j.mrfmmm.2011.06.005.

[10] F.M. Stewart, D.M. Gordon, B.R. Levin, Fluctuation analysis: the probability distribution of the number of mutants under different conditions, Genetics 124 (1) (1990) 175–185, https://doi.org/10.1093/genetics/124.1.175.

[11] F.M. Stewart, Fluctuation analysis: the effect of plating efficiency, Genetica 84 (1) (1991) 51–55, https://doi.org/10.1007/BF00123984.

[12] Q. Zheng, Progress of a half century in the study of the Luria-Delbrück distribution, Math. Biosci. 162 (1–2) (1999) 1–32, https://doi.org/10.1016/S0025-5564(99)00045-0.

[13] P. Armitage, The statistical theory of bacterial populations subject to mutation, J. R. Stat. Soc.: Ser. B (Methodol.) 14 (1) (1952) 1–33, https://doi.org/10.1111/j.2517-6161.1952.tb00098.x.

[14] Q. Zheng, Toward a unique definition of the mutation rate, Bull. Math. Biol. 79 (4) (2017) 683–692, https://doi.org/10.1007/s11538-017-0247-8.

[15] N.T.J. Bailey. The elements of stochastic processes with applications to the natural sciences, 1st edition, John Wiley & Sons Inc,, 1964.

[16] K.S. Crump, D.G. Hoel, Mathematical models for estimating mutation rates in cell populations, Biometrika 61 (2) (1974) 237–252, https://doi.org/10.1093/biomet/61.2.237.

[17] P.L. Foster, Mechanisms of stationary phase mutation: a decade of adaptive mutation, Annu. Rev. Genet. 33 (1) (1999) 57–88, https://doi.org/10.1146/annurev.genet.33.1.57.

[18] L. Loewe, High deleterious genomic mutation rate in stationary phase of *Escherichia coli*, Science 302 (5650) (2003) 1558–1560, https://doi.org/10.1126/science.1087911.

[19] C.H. Corzett, M.F. Goodman, S.E. Finkel, Competitive fitness during feast and famine: How SOS DNA polymerases influence physiology and evolution in *Escherichia coli*, Genetics 194 (2) (2013) 409–420, https://doi.org/10.1534/genetics.113.151837.

[20] M.G. Reynolds, Compensatory evolution in rifampin-resistant *Escherichia coli*, Genetics 156 (4) (2000) 1471–1481, https://doi.org/10.1093/genetics/156.4.1471.

[21] J. Cairns, J. Overbaugh, S. Miller, The origin of mutants, Nature 335 (6186) (1988) 142–145, https://doi.org/10.1038/335142a0.

[22] G.R. Hoffmann, C.L. Gray, P.B. Lange, C.I. Marando, A source of artifact in the *lacZ* reversion assay in *Escherichia coli*, Mutat. Res. /Genet. Toxicol. Environ. Mutagen. 784–785 (2015) 23–30, https://doi.org/10.1016/J.MRGENTOX.2015.04.008.

[23] H.B. Newcombe, Delayed phenotypic expression of spontaneous mutations in *Escherichia coli*, Genetics 33 (5) (1948) 447–476, https://doi.org/10.1093/genetics/33.5.447.

[24] L. Sun, H.K. Alexander, B. Bogos, D.J. Kiviet, M. Ackermann, S. Bonhoeffer, Effective polyploidy causes phenotypic delay and influences bacterial evolvability, PLOS Biol. 16 (2) (2018), e2004644, https://doi.org/10.1371/journal.pbio.2004644.

[25] Q. Zheng, A note on plating efficiency in fluctuation experiments, Math. Biosci. 216 (2) (2008) 150–153, https://doi.org/10.1016/j.mbs.2008.09.002.

[26] Q. Zheng, Comparing mutation rates under the Luria-Delbrück protocol, Genetica 144 (3) (2016) 351–359, https://doi.org/10.1007/s10709-016-9904-3.

[27] Q. Zheng, rSalvador: an R package for the fluctuation experiment, G3: Genes, Genomes, Genetics 7 (12) (2017) 3849–3856, https://doi.org/10.1534/g3.117.300120.

[28] W.T. Ma, G. v. Sandri, S. Sarkar, Analysis of the Luria-Delbrück distribution using discrete convolution powers, J. Appl. Probab. 29 (2) (1992) 255–267, https://doi.org/10.2307/3214564.

[29] S. Sarkar, W.T. Ma, G. v. Sandri, On fluctuation analysis: a new, simple and efficient method for computing the expected number of mutants, Genetica 85 (2) (1992) 173–179, https://doi.org/10.1007/BF00120324.

[30] Q. Zheng, Statistical and algorithmic methods for fluctuation analysis with SALVADOR as an implementation, Math. Biosci. 176 (2) (2002) 237–252, https://doi.org/10.1016/S0025-5564(02)00087-1.

[31] G.J. Crane, S.M. Thomas, M.E. Jones, A modified Luria-Delbrück fluctuation assay for estimating and comparing mutation rates, Mutat. Res. - Fundam. Mol. Mech. Mutagen. 354 (2) (1996) 171–182, https://doi.org/10.1016/0027-5107(96)00009-7.

[32] M.E. Jones, Accounting for plating efficiency when estimating spontaneous mutation rates, Mutat. Res. /Environ. Mutagen. Relat. Subj. 292 (2) (1993) 187–189, https://doi.org/10.1016/0165-1161(93)90146-Q.

[33] M.E. Jones, An algorithm accounting for plating efficiency in estimating spontaneous mutation rates, Comput. Biol. Med. 23 (6) (1993) 455–461, https://doi.org/10.1016/0010-4825(93)90093-G.

[34] M.E. Jones, Luria-Delbrück fluctuation experiments; accounting simultaneously for plating efficiency and differential growth rate, J. Theor. Biol. 166 (3) (1994) 355–363, https://doi.org/10.1006/jtbi.1994.1032.

[35] P. Gerrish, A simple formula for obtaining markedly improved mutation rate estimates, Genetics 180 (3) (2008) 1773–1778, https://doi.org/10.1534/genetics.108.091777.

[36] A.L. Koch, Mutation and growth rates from Luria-Delbrück fluctuation tests, Mutat. Res. - Fundam. Mol. Mech. Mutagen. 95 (2–3) (1982) 129–143, https://doi.org/10.1016/0027-5107(82)90252-4.

[37] B. Mandelbrot, A population birth-and-mutation process, I: explicit distributions for the number of mutants in an old culture of bacteria, J. Appl. Probab. 11 (3) (1974) 437–444, https://doi.org/10.2307/3212688.

[38] W.P. Angerer, A note on the evaluation of fluctuation experiments, Mutat. Res. - Fundam. Mol. Mech. Mutagen. 479 (1–2) (2001) 207–224, https://doi.org/10.1016/S0027-5107(01)00203-2.

[39] Q. Zheng, On Bartlett's formulation of the Luria-Delbrück mutation model, Math. Biosci. 215 (1) (2008) 48–54, https://doi.org/10.1016/j.mbs.2008.05.005.

[40] Q. Zheng, A new discrete distribution induced by the Luria-Delbrück mutation model, Statistics 44 (5) (2010) 529–540, https://doi.org/10.1080/02331880903236868.

[41] Q. Zheng, A second look at the final number of cells in a fluctuation experiment, J. Theor. Biol. 401 (2016) 54–63, https://doi.org/10.1016/j.jtbi.2016.04.027.

[42] B. Ycart, N. Veziris, Unbiased estimation of mutation rates under fluctuating final counts, PLoS ONE 9 (7) (2014), https://doi.org/10.1371/journal.pone.0101434.

[43] W.P. Angerer, An explicit representation of the Luria-Delbrück distribution, J. Math. Biol. 42 (2) (2001) 145–174, https://doi.org/10.1007/s002850000053.

[44] A. Dewanji, E.G. Luebeck, S.H. Moolgavkar, A generalized Luria-Delbrück model, Math. Biosci. 197 (2) (2005) 140–152, https://doi.org/10.1016/j.mbs.2005.07.003.

[45] D.G. Kendall, Birth-and-death processes, and the theory of carcinogenesis, Biometrika 47 (1/2) (1960) 13, https://doi.org/10.2307/2332953.

[46] Q. Zheng, Estimation of rates of non-neutral mutations when bacteria are exposed to subinhibitory levels of antibiotics, Bull. Math. Biol. 84 (11) (2022) 1–18, https://doi.org/10.1007/s11538-022-01085-5.

[47] A. Gillet-Markowska, G. Louvel, G. Fischer, bz-rates: a web tool to estimate mutation rates from fluctuation analysis, G3: Genes, Genomes, Genetics 5 (11) (2015) 2323–2327, https://doi.org/10.1534/g3.115.019836.

[48] A. Mazoyer, R. Drouilhet, S. Despréaux, B. Ycart, Flan: an R package for inference on mutation models, R Journal 9 (1) (2017) 334–351, https://doi.org/10.32614/rj-2017-029.

[49] E.A. Radchenko, R.J. McGinty, A.Y. Aksenova, A.J. Neil, S.M. Mirkin, Quantitative analysis of the rates for repeat-mediated genome instability in a yeast experimental system, Genome Instability 1672 (2018) 421–438, https://doi.org/10.1007/978-1-4939-7306-4_29.

[50] B.M. Hall, C.X. Ma, P. Liang, K.K. Singh, Fluctuation analysis calculator: a web tool for the determination of mutation rate using Luria-Delbrück fluctuation analysis, Bioinformatics 25 (12) (2009) 1564–1565, https://doi.org/10.1093/bioinformatics/btp253.

[51] C.T. H. Barna, Mutation rates of *Escherichia coli* with different balanced growth rates: a new fluctuation test protocol and phenotypic lag adjustments, PhD Thesis, University of Waterloo, Waterloo, Ontario, Canada (2020).

[52] Q. Zheng, New algorithms for Luria-Delbrück fluctuation analysis, Math. Biosci. 196 (2) (2005) 198–214, https://doi.org/10.1016/j.mbs.2005.03.011.

[53] A.H. Melnyk, A. Wong, R. Kassen, The fitness costs of antibiotic resistance mutations, Evolut. Appl. 8 (3) (2015) 273–283, https://doi.org/10.1111/eva.12196.

[54] M.J. Wiser, R.E. Lenski, A comparison of methods to measure fitness in *Escherichia coli*, PLoS ONE 10 (5) (2015) 1–11, https://doi.org/10.1371/journal.pone.0126210.

[55] E. Curti, J.P. McDonald, S. Mead, R. Woodgate, Dna polymerase switching: Effects on spontaneous mutagenesis in *Escherichia coli*, Mol. Microbiol. 71 (2) (2009) 315–331, https://doi.org/10.1111/j.1365-2958.2008.06526.x.

[56] J.E. Barrick, M.R. Kauth, C.C. Streliff, R.E. Lenski, *Escherichia coli rpoB* mutants have increased evolvability in proportion to their fitness defects, Mol. Biol. Evol. 27 (6) (2010) 1338–1347, https://doi.org/10.1093/molbev/msq024.

[57] Q. Qi, G.M. Preston, R.C. Maclean, Linking system-wide impacts of rna polymerase mutations to the fitness cost of rifampin resistance in *Pseudomonas aeruginosa*, mBio 5 (6) (2014), https://doi.org/10.1128/mBio.01562-14.

[58] J. Sun, D. Zhu, J. Xu, R. Jia, S. Chen, M. Liu, X. Zhao, Q. Yang, Y. Wu, S. Zhang, Y. Liu, L. Zhang, Y. Yu, Y. You, M. Wang, A. Cheng, Rifampin resistance and its fitness cost in *Riemerella anatipestifer*, BMC Microbiol. 19 (1) (2019) 1–13, https://doi.org/10.1186/s12866-019-1478-7.

[59] G. Brandis, M. Wrande, L. Liljas, D. Hughes, Fitness-compensatory mutations in rifampicin-resistant RNA polymerase, Mol. Microbiol. 85 (1) (2012) 142–151, https://doi.org/10.1111/j.1365-2958.2012.08099.x.

[60] A.R. Tuttle, N.D. Trahan, M.S. Son, Growth and maintenance of *Escherichia coli* laboratory strains, Curr. Protoc. 1 (1) (2021) 1–13, https://doi.org/10.1002/cpz1.20.

[61] N. Nagar, N. Ecker, G. Loewenthal, O. Avram, D. Ben-Meir, D. Biran, E. Ron, T. Pupko, Harnessing machine learning to unravel protein degradation in *Escherichia coli*, mSystems 6 (1) (2021) 2, https://doi.org/10.1128/mSystems.01296-20.

[62] G.E. Kissling, D.W. Grogan, J.W. Drake, Confounders of mutation-rate estimators: Selection and phenotypic lag in *Thermus thermophilus*, Mutat. Res. - Fundam. Mol. Mech. Mutagen 749 (1-2) (2013) 16–20, https://doi.org/10.1016/j.mrfmmm.2013.07.006.

[63] J.U. Dimude, A. Stockum, S.L. Midgley-Smith, A.L. Upton, H.A. Foster, A. Khan, N. J. Saunders, R. Retkute, C.J. Rudolph, The consequences of replicating in the wrong orientation: bacterial chromosome duplication without an active replication origin, mBio 6 (6) (2015) 1–13, https://doi.org/10.1128/mBio.01294-15.

[64] M. Carballo-Pacheco, M.D. Nicholson, E.E. Lilja, R.J. Allen, B. Waclaw, Phenotypic delay in the evolution of bacterial antibiotic resistance: mechanistic models and their implications, PLoS Comput. Biol. 16 (5) (2020) 1–24, https://doi.org/10.1371/journal.pcbi.1007930.

[65] L. Boe, T. Tolker-Nielsen, K.M. Eegholm, H. Spliid, A. Vrang, Fluctuation analysis of mutations to nalidixic acid resistance in *Escherichia coli*, J. Bacteriol. 176 (14) (1994) 4463, https://doi.org/10.1128/JB.176.14.4463-4463.1994.

[66] S.S. Wilks, The large-sample distribution of the likelihood ratio for testing composite hypotheses, Ann. Math. Stat. 9 (1) (1938) 60–62, https://doi.org/10.1214/aoms/1177732360.

[67] S. Fred, Getting started with yeast, Methods Enzymol. 350 (2002) 3–41, https://doi.org/10.1016/S0076-6879(02)50954-X.

[68] M. Martin-Perez, J. Villén, Determinants and regulation of protein turnover in yeast, Cell Syst. 5 (3) (2017) 283–294.e5, https://doi.org/10.1016/j.cels.2017.08.008.

[69] R. Christiano, N. Nagaraj, F. Fröhlich, T.C. Walther, Global proteome turnover analyses of the yeasts *S. cerevisiae* and *S. pombe*, Cell Rep. 9 (5) (2014) 1959–1965, https://doi.org/10.1016/j.celrep.2014.10.065.

[70] A. Frenoy, S. Bonhoeffer, Death and population dynamics affect mutation rate estimates and evolvability under stress in bacteria, PLoS Biol. 16 (5) (2018), e2005056, https://doi.org/10.1371/journal.pbio.2005056.

[71] X. Wu, H. Zhu, Fast maximum likelihood estimation of mutation rates using a birth-death process, J. Theor. Biol. 366 (2015) 1–7, https://doi.org/10.1016/j.jtbi.2014.11.009.

[72] I.A. Rodriguez-Brenes, D. Wodarz, N.L. Komarova, Cellular replication limits in the Luria-Delbrück mutation model, Phys. D: Nonlinear Phenom. 328- 329 (2016) 44–51, https://doi.org/10.1016/j.physd.2016.04.007.

[73] Q. Zheng, A Bayesian two-level model for fluctuation assay, Genetica 139 (11–12) (2011) 1409–1416, https://doi.org/10.1007/s10709-012-9639-8.

[74] M.N. Ragheb, M.K. Thomason, C. Hsu, P. Nugent, J. Gage, A.N. Samadpour, A. Kariisa, C.N. Merrikh, S.I. Miller, D.R. Sherman, H. Merrikh, Inhibiting the evolution of antibiotic resistance, Mol. Cell (2018) 206–221, https://doi.org/10.1016/j.molcel.2018.10.015.

[75] I. ElMeouche, M.J. Dunlop, Heterogeneity in efflux pump expression predisposes antibiotic-resistant cells to mutation, Science 362 (6415) (2018) 686–690, https://doi.org/10.1126/science.aar7981.

[76] T.M. Nye, L.A. van Gijtenbeek, A.G. Stevens, J.W. Schroeder, J.R. Randall, L. A. Matthews, L.A. Simmons, Methyltransferase DnmA is responsible for genome-wide n6-methyladenosine modifications at non-palindromic recognition sites in *Bacillus subtilis*, Nucleic Acids Res. 48 (10) (2021) 5332–5348, https://doi.org/10.1093/NAR/GKAA266.

[77] D.A. Kessler, H. Levine, Large population solution of the stochastic Luria-Delbrück evolution model, Proc. Natl. Acad. Sci. 110 (29) (2013) 11682–11687, https://doi.org/10.1073/pnas.1309667110.

[78] D.A. Kessler, H. Levine, Scaling solution in the large population limit of the general asymmetric stochastic Luria-Delbrück evolution process, J. Stat. Phys. 158 (4) (2015) 783–805, https://doi.org/10.1007/s10955-014-1143-3.

[79] T. Antal, P.L. Krapivsky, Exact solution of a two-type branching process: models of tumor progression, J. Stat. Mech.: Theory Exp. 2011 (08) (2011) P08018, https://doi.org/10.1088/1742-5468/2011/08/P08018.

[80] N.L. Komarova, L. Wu, P. Baldi, The fixed-size Luria-Delbrück model with a nonzero death rate, Math. Biosci. 210 (1) (2007) 253–290, https://doi.org/10.1016/j.mbs.2007.04.007.